Water Resources Research

RESEARCH ARTICLE
10.1029/2023WR036520

Biocrusts Critical Regulation of Soil Water Vapor Transport (Diffusion, Sorption, and Late-Stage Evaporation) in Drylands

Fuhai Sun[1], Bo Xiao[1,2,3], Giora J. Kidron[4], and Joshua Heitman[5]

[1]Key Laboratory of Arable Land Conservation in North China, Ministry of Agriculture and Rural Affairs/College of Land Science and Technology, China Agricultural University, Beijing, China, [2]State Key Laboratory of Soil Erosion and Dryland Farming on the Loess Plateau, Institute of Soil and Water Conservation, Chinese Academy of Sciences and Ministry of Water Resources, Yangling, China, [3]Breeding Base for State Key Laboratory of Land Degradation and Ecological Restoration in Northwestern China/Key Laboratory of Restoration and Reconstruction of Degraded Ecosystems in Northwestern China of Ministry of Education, Ningxia University, Yinchuan, China, [4]Institute of Earth Sciences, The Hebrew University of Jerusalem, Jerusalem, Israel, [5]Department of Crop and Soil Sciences, North Carolina State University, Raleigh, NC, USA

Abstract Soil surface cover is one of the most critical factors affecting soil water vapor transport, especially in drylands where water is limited, and the water movement occurs predominantly in the form of vapor instead of liquid. Biocrusts are an important living ground cover of dryland soils and play a vital role in modifying near-surface soil properties and maintaining soil structure. The role of biocrusts in mediating soil water vapor transport during daytime water evaporation and nighttime condensation remains unclear. We investigated the differences in vapor diffusion properties, vapor adsorption capacity, and water evaporation between bare soil and three types of biocrusts (cyanobacterial, cyanobacterial-moss mixed, and moss crusts) in the Chinese Loess Plateau. Our results showed that the three types of biocrusts had 5%–39% higher vapor diffusivity than bare soil. At the same level of ambient relative humidity and temperature, the initial vapor adsorption rates and cumulative adsorption amounts of the biocrusts were 10%–70% and 11%–85% higher than those of bare soil, respectively. Additionally, the late-stage evaporation rate of cyanobacterial-, cyanobacterial-moss mixed-, and moss-biocrusts were 31%–217%, 79%–492%, and 146%–775% higher than that of bare soil, respectively. The effect of biocrusts on increasing vapor transport properties was attributed to the higher soil porosity, clay content, and specific surface area induced by the biocrust layer. All of these modifications caused by biocrusts on surface soil vapor transport properties suggest that biocrusts play a vital role in reshaping surface soil water and energy balance in drylands.

Key Points:

- Biocrusts increase water vapor diffusion properties, water vapor adsorption amount, and cumulative evaporation amount
- Modified soil properties of biocrust are a key factor influencing water vapor flux
- Reshaped vapor transport properties of biocrust control soil water and energy balance

Supporting Information:

Supporting Information may be found in the online version of this article.

Correspondence to:

B. Xiao,
xiaobo@cau.edu.cn

Citation:

Sun, F., Xiao, B., Kidron, G. J., & Heitman, J. (2024). Biocrusts critical regulation of soil water vapor transport (diffusion, sorption, and late-stage evaporation) in drylands. *Water Resources Research*, *60*, e2023WR036520. https://doi.org/10.1029/2023WR036520

Received 26 OCT 2023
Accepted 14 JUN 2024

Author Contributions:

Conceptualization: Fuhai Sun
Formal analysis: Fuhai Sun, Bo Xiao
Funding acquisition: Bo Xiao
Investigation: Fuhai Sun
Methodology: Fuhai Sun
Project administration: Bo Xiao
Resources: Fuhai Sun
Supervision: Bo Xiao
Writing – original draft: Fuhai Sun, Bo Xiao
Writing – review & editing: Bo Xiao, Giora J. Kidron, Joshua Heitman

1. Introduction

Drylands encompassing hyper-arid, arid, semi-arid, and dry sub-humid regions, collectively occupy ~41% of the Earth's land surface, sustaining ~38% of world's population, and holding ~25% of global soil organic carbon (J. F. Reynolds et al., 2007). Due to the sparse vegetation, limited precipitation, and intense evaporation, dryland ecosystems are fragile and sensitive to global climate change and desertification (Mao et al., 2018). In drylands, soils have relatively low moisture, and water transport occurs predominantly in vapor form instead of liquid (Huang et al., 2016). Soil vapor transport plays a critical role in water and energy balances of near-surface soil layers, and therefore has a substantial impact on multiple processes directly related to ecosystem structure and functioning, such as biological activity, plant productivity, and nutrient concentration (Berdugo et al., 2020). Most notably, climate projections indicate that ongoing global warming will cause drylands to become hotter and drier in the late twenty-first century, which in turn may enhance soil vapor transport (IPCC, 2021). Consequently, it is essential to investigate soil vapor transport properties for further understanding the exchange of water and energy in dryland ecosystems. Soil vapor transport is influenced by the combination of soil texture, porosity, structure, and especially surface cover (Arthur et al., 2015), and biocrusts directly impact each of these factors. Thus, biocrusts are also likely to play a major role in impacting soil ecohydrological processes (S. L. Li et al., 2022a).

Biocrusts are complex communities of living organisms dwelling on or within the uppermost few millimeters (or even centimeters) of the soil surface, and are widely distributed in the interspaces between sparse vegetation,

covering about 14% of China's dryland soil and over 12% of global terrestrial surface (Qiu et al., 2023; Rodríguez-Caballero et al., 2018; Weber et al., 2022). These soil surface communities are composed of photoautotrophic (e.g., cyanobacteria, algae, liverworts, lichens, and bryophytes) plus heterotrophic organisms (e.g., bacteria, archaea, and fungi) in varying proportions, as well as soil particles that are aggregated through the presence and activity of the biota (Xiao et al., 2022). Generally, the external morphology of biocrusts could produce a bumpy soil surface with numerous small depressions and mounds, thereby increasing surface roughness (Thomas & Dougill, 2007). The rough surface microtopography of biocrusts is beneficial to capture and retain fine sediment mobilized by wind and surface runoff. Thus, hollows will be filled with fine particles (clay and silt), and the biotic components in biocrusts (such as bacteria, fungi, and cyanobacteria) could secrete extracellular polysaccharide compounds that glue and bind the entrapped fine particles together (Chock et al., 2019; Xiao, Sun, Hu, & Kidron, 2019) and further stabilize soil surface, thereby altering soil particle distribution. The enriched microbial communities of biocrusts could also promote the biological weathering of the mineral component to generate fine particles (R. Y. Chen et al., 2009). Moreover, the biocrusts could enhance surface resistance, effectively diminish the energy of runoff, impede transport of sediment, and reduce the detachment of soil particles, which ultimately results in protecting the fine particles from erosion (Q. Guo et al., 2023; R. Reynolds et al., 2001). As crucial biotic components inhabiting the soil-atmosphere boundary, biocrusts are widely recognized as ecosystem engineers and play pivotal roles in reshaping surface soil properties and multifunctionality (Bowker et al., 2018), such as boosting soil stability (Felde et al., 2018; Rossi et al., 2018), improving soil structure (Sun, Xiao, Li, et al., 2023), retarding wind erosion (Bu et al., 2015; Faist et al., 2017), improving soil aeration (Sun, Xiao, Kidron, & Markus, 2023), altering albedo and energy balance (Rutherford et al., 2017; Xiao & Bowker, 2020), and promoting microbial diversity (Maier et al., 2018). Therefore, it is widely accepted that biocrusts are capable of promoting ecological restoration through mediating the hydrological, biological, and ecological processes (Heredia-Velásquez et al., 2023). Owing to the limited soil water resources in dryland ecosystems, several biocrust studies have concentrated on the interactions between biocrusts and liquid water, for example, by quantifying how biocrusts can regulate soil water infiltration and water retention (Sun et al., 2021; Xiao, Sun, Yao, et al., 2019). Effects of biocrusts on vapor transport has been far less studied but may also be an important consideration.

Evaporation, subsequent vapor transport, and vapor sorption play crucial roles in the overall water flux near the soil surface, especially in arid and semiarid areas (Deb et al., 2011). Soil vapor transport across pore space in topsoil, which may subsequently escape to the atmosphere, takes place predominately by diffusion (Deol et al., 2012; Penman, 1940). Vapor diffusion at the soil surface is controlled by two main conditions, namely vapor pressure (moisture) and temperature gradients (Cass et al., 1984). Generally, vapor diffusion moves water from moist soil to dry soil, and from the warmer to the cooler region (Heitman, Horton, et al., 2008; Jabro, 2009). The higher the gradient, the faster the diffusion and the greater the vapor flux during a given period. Moreover, the vapor diffusion is strongly influenced by the physical properties of the soil, such as soil texture, bulk density, and total porosity. Although vapor diffusion is one of the critical components of total water flux in the unsaturated zone, comparatively few studies focused on the effects of biocrusts on the mechanism of vapor diffusion.

Soil vapor adsorption is another crucial contributor to the water cycle in drylands (Schneider & Goss, 2012). Soil vapor adsorption takes place when the vapor pressure of the atmosphere is higher than that of soil air, resulting in vapor diffusion from the atmosphere toward the soil (Akin & Likos, 2017). Soil vapor adsorption generally occurs in three stages: (a) water vapor monolayer adsorption, which occurs when relative humidity (RH) ranges from near 0 to 0.2 (Newman, 1983; Quirk & Murray, 1999); (b) water vapor multiple layer adsorption, which also develops when RH ranges from 0.2 to 0.6 (Arthur et al., 2018; Quirk & Murray, 1999); and (c) capillary condensation, which occurs when RH is above ∼0.6 (Arthur et al., 2016). During the first adsorption stage, mineral soil adsorbs water molecules through cation and particle surface hydration, and hydrogen bonding of water molecules with the hydrophilic functional groups on soil organic matter (Lu & Khorshidi, 2015). When the monolayer is formed, the previous adsorbed water molecules act as new sorption sites to adsorb additional water molecules via hydrogen bonding to form multiple layers of liquid water (Cheng et al., 2019). During the last stage, the capillary condensation is the primary form of soil hydration, although the water molecules still in vapor form, water film begin to demonstrate liquid-like nature (Arthur et al., 2016). This process is dominated by external surface and mesopore volume, because water vapor condensation can occur on the open surfaces and within the mesoporous (Tuller et al., 1999). Soil vapor adsorption capacity depends not only on micrometeorological conditions, but also on soil properties. Vapor adsorption capacity increases with increasing clay content, specific

surface area, and cation exchange capacity (C. Chen et al., 2021; Song et al., 2022). Moreover, the vapor adsorption of the biocrusts is deeply affected by soil pore structure and biological components in the field. Currently, most studies explore the effects of biocrusts on vapor adsorption through sieved soil samples, and thus cannot obtain comprehensive information about the biocrusts' role in reshaping soil vapor adsorption.

Soil water evaporation is another important related process governing the terrestrial vapor flux in dryland ecosystems, which affects water availability and vegetation growth, and restoration (N. Chen et al., 2018; D. D. Liu & She, 2020). Soil evaporation processes has been often separated into three stages: high rate (stage I), falling rate (stage II), and low and constant rate stage (stage III). Initial evaporation (stage I) occurs at the soil surface when soil conditions are relatively wet and is controlled by the atmospheric evaporative demand. During late-stage evaporation (stages II and III), the evaporation zone shifts from soil surface to subsurface and generates a dry surface layer, which is mainly modulated by soil properties (Heitman, Xiao, et al., 2008). Specifically, the late-stage evaporation occurs in a narrow evaporation zone at the bottom boundary of the dry surface layer (Yamanaka et al., 1998), and the vapor diffusion predominating in the profile above the evaporation zone. Moreover, due to the limited rainfall and water shortages in semi-arid and arid areas, evaporation usually begins at Stage II and water transport is mainly as vapor diffusion (S. L. Li et al., 2022b). It is widely recognized that biocrusts have a profound impact on soil evaporation through their biotic components, such as the composition and coverage of biocrusts (Kidron, Fischer, & Xiao, 2022; S. L. Li et al., 2022b), and modified physical structure, such as the roughness, porosity, stability, and hydrophobicity (Chamizo et al., 2016). The impact of biocrusts on soil evaporation is quite controversial in the literature, being either facilitative (Kidron & Tal, 2012; S. L. Li & Xiao, 2022; S. L. Li et al., 2022b) or inhibitive (Jiang et al., 2018; Kakeh et al., 2021; D. D. Liu & She, 2020). Biocrusts affect soil evaporation mostly by influencing soil texture and structure, water holding capacity, and surface color. Soil evaporation may be increased by biocrusts through the following mechanisms: (a) Biocrusts may improve the water holding capacity and increase the amount of water available to be evaporated (S. L. Li et al., 2022b). (b) The soil temperature of biocrusts may rise due to their darker surface color, lower surface albedo, and higher solar radiation absorption (Xiao & Bowker, 2020), and thus are expected to have increased evaporation potential (Kidron & Tal, 2012). However, some studies attribute the reduction of evaporation by biocrusts to mulch-like surface-shading properties (Mücher et al., 1988), while others claim that biocrusts may reduce available water vapor pathways through the swelling of organisms when wet and ultimately decreasing evaporation (Fischer et al., 2010; Rodríguez-Caballero et al., 2015). Further work is needed to better understand how biocrusts regulate soil evaporation, especially for the late-stage evaporation process that is controlled by vapor diffusion.

Investigation of vapor exchange at the soil surface is essential for better quantifying and ultimately improving the understanding and prediction of surface soil water balance in drylands. In this study, we hypothesized that the presence of biocrusts would affect soil vapor transport through their effects on soil physicochemical properties. Based on this general hypothesis, a series of soil vapor transport experiments were conducted on three types of biocrusts (cyanobacterial crusts, cyanobacterial-moss mixed crusts, and moss crusts) and bare soil. Measurements were conducted at the semiarid climate of the Chinese Loess Plateau, where *Lyngbya allorgei* and *Bryum argenteum* (R. Brown) B.S.G. are the dominated cyanobacteria and moss species, respectively (X. R. Li et al., 2021). The specific objectives of our study were to: (a) quantify biocrust effects on surface soil vapor transport properties (vapor diffusion, vapor adsorption, and water evaporation) and (b) connect the biocrust influences on soil vapor transport to the associated changes biocrusts produce in soil physicochemical properties. These results can provide new insights as to type effects biocrusts have on soil water transport and thereby support a better understanding of the critical role biocrusts play in dryland hydrology and ecohydrology.

2. Materials and Methods

2.1. Study Area

The study was conducted in a vegetation restoration area at the Liudaogou watershed (38°46′–38°51′N, 110°21′–110°21′E; Figures 1a and 1b), which is located in Shenmu County, Shaanxi Province, China. The watershed is a typical hilly region with numerous gullies of the northern Chinese Loess Plateau, which covers an area of 6.9 km^2 and ranges in altitude from 1,081 to 1,274 m above sea level. It is characterized by a typical semiarid continental monsoon climate with a mean annual precipitation of 454 mm, mostly falling as rain during hot summers (Xiao & Bowker, 2020). The mean annual temperature is 8.4°C, which ranges from −9.7°C (December–February) in

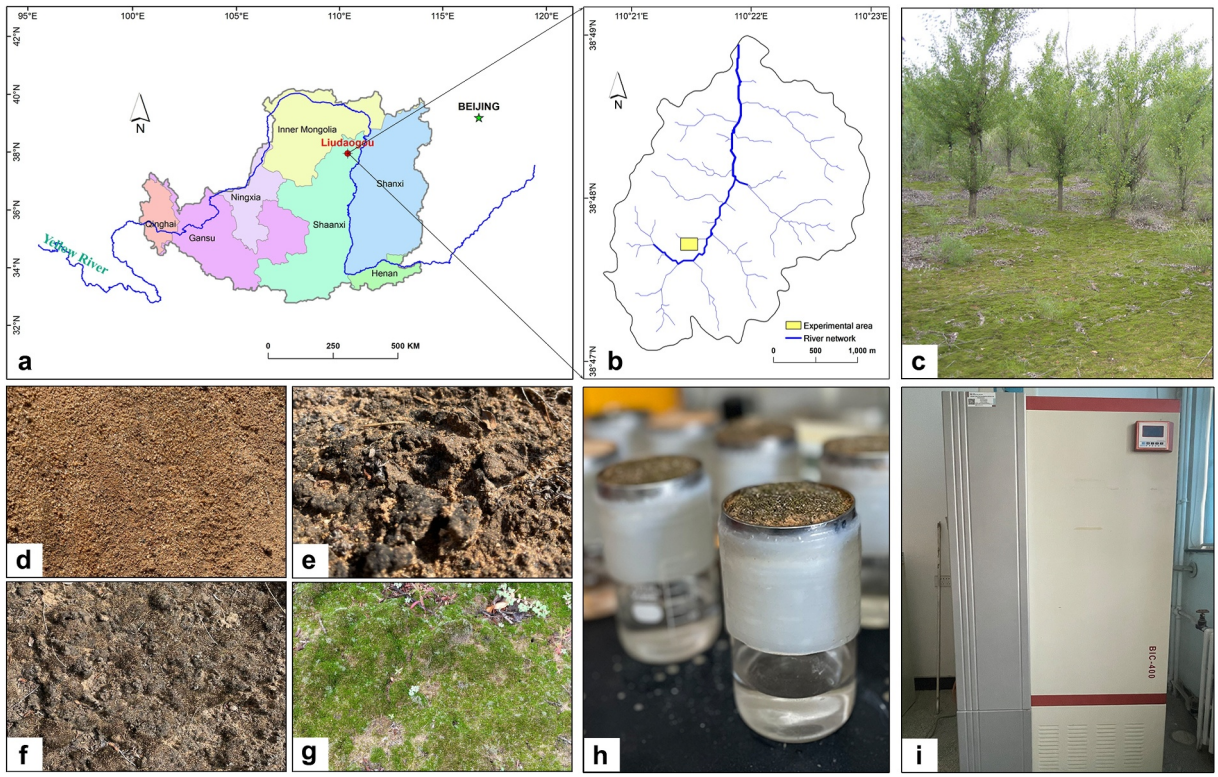

Figure 1. (a) Location of the Liudaogou watershed, (b) experimental area, (c) representative landscape with biocrusts, (d) bare aeolian sand, (e) cyanobacterial biocrusts, (f) cyanobacterial and moss mixed biocrusts, (g) moss biocrusts, (h) test device for water vapor diffusion measurements, and (i) artificial climate incubator.

winter to 23.7°C in summer (June–August) (Xiao et al., 2014). The average annual potential evaporation is ~1,337 mm (Sun, Xiao, Kidron, & Heitman, 2022). The mean air RH is 47% with the lowest observed values approaching 9% (Xiao, Sun, Hu, & Kidron, 2019). The soil is classified as a Psamments (specifically an aeolian sandy soil) with a high proportion of sand (>90%) following the taxonomic classification of the USDA (Sun, Xiao, Li, et al., 2023). The watershed is situated close to the center of the "Water-Wind Erosion Crisscross Region" of the Loess Plateau and previously suffered both severe wind and water erosion (i.e., up to 10,000 t km^{-2} yr^{-1}) due to the sparse vegetation cover (Bu et al., 2015).

Over the past decades, intensive ecological restoration programs have taken place, such as planting numerous native shrubs and converting degraded farmlands and barren lands to grasslands, shrubland, or even forests. The common plants in this watershed include *Bothriochloa ischaemum* (Linn.) Keng., *Medicago sativa* Linn., *Artemisia ordosica* Krasch., *Caragana Korshinskii* Kom., *Cotoneaster horizontalis* Dcne., and *Lespedeza davurica* (Laxm.) Schindl (Sun, Xiao, Kidron, & Heitman, 2022). Biocrusts are ubiquitous across fallow land, grassland, shrubland, and woodland, averaging 30% cover and sometimes up to 70%–80% cover across the watershed (Figure 1c; Xiao, Sun, Hu, & Kidron, 2019). Within the watershed, the species of cyanobacterial and moss crusts were observed by microscopy. Specifically, biocrust species are variable and may be diverse, but in most areas they are dominated by cyanobacteria of *Lyngbya allorgei*, *Oscillatoria granulata*, *Microcolus paludosus* and *Phormidium angustissimum* and mosses of *Bryum argenteum* (R. Brown) B.S.G. and *Didymodon vinealis* (Brid.) Zander, as well as their mixtures (Figure S1 in Supporting Information S1).

2.2. Experimental Design and Soil Sampling

Four treatments (i.e., soil surface conditions) were used for the study. These included: (a) bare soil (aeolian sandy soil without biocrusts; Figure 1d); (b) cyanobacterial crusts (cyano crusts, which have ~90% of cyanobacterial cover; Figure 1e); (c) cyanobacterial and moss mixed crusts (mixed crusts, in which cyanobacterial and moss cover were both ~50%; Figure 1f); and (d) moss crusts (moss cover is ~90%; Figure 1g). Generally, the biocrusts

were naturally colonized on the fixed aeolian sand, being distributed in the interspaces between vegetation patches. In contrast, the bare soil was located away from the vegetation, being exposed to soil erosion.

Four types of characterizations were utilized to compare treatments: (a) biocrusts and bare soil sampling and physicochemical property measurements; (b) soil vapor diffusion experiments under different temperatures and RH; (c) measurements of soil vapor adsorption processes; and (d) measurements of soil evaporation processes from saturation to dry in simulated evaporation experiments.

2.3. Sampling and Measurements of Soil Properties

Within the experimental area, for sample collection, the biocrusts and adjacent bare soil plots (1 m × 1 m) were randomly selected considering similar topological conditions (i.e., slope and aspect). For each treatment, five replicate plots (1 m × 1 m) were selected at 1-m spacing to minimize variations in soil texture, biocrust coverage (>90%) and species, resulting in a total of 20 plots. Before sampling, digital photographs were taken of the plots for further analysis of biocrust coverage. Meanwhile, water drop penetration time was tested using the method described in Lichner et al. (2012).

In each plot, three Petri dishes (9 cm diameter, 2 cm height) were used to collect the biocrust layer and underlying soil for measuring total biomass, biocrust thickness, and chlorophyll *a* content, respectively. Additionally, seven stainless steel cylinders (2 cm height, 60 cm^3 volume) were used to extract intact soil samples from each plot for bulk density, saturated water content, field capacity, water repellency index, vapor diffusion, vapor adsorption, and water evaporation measurements, respectively. Finally, bulk soil samples were collected from the 0–2 cm depth in each plot. These bulk soil samples were air-dried and sieved through 2 and 0.149 mm mesh sieves for soil physicochemical analysis, which included soil particle size distribution, soil pH, specific surface area, and organic matter content.

The biocrust coverage of each plot was analyzed with ImageJ (Wayne Rasband, National Institutes of Health), as described in Sun, Xiao, and Kidron (2022). The surface roughness of the biocrust and bare soil plots was measured with the chain method (Jester & Klik, 2005). In the laboratory, the biocrust thickness was determined using a digital Vernier caliper. Then, the biotic component of the biocrust layer was carefully separated from the underlying soil particles with water through a 2-mm sieve and dried at 65°C for 24 hr to measure the dry total biomass (Xiao, Sun, Hu, & Kidron, 2019). The Chlorophyll *a* content was determined through a UV–Vis spectrophotometer (DR 5000, Hach Company, USA). Nitrogen adsorption/desorption analysis via a specific surface area analyzer (3H-200PM, BeiShiDe Instrument, China) was conducted to calculate the soil specific surface area by the Brunauer-Emmett-Tell (BET) method. Air-dried soil samples were automatically degassed at 150°C for ∼12 hr in N_2 flowing tubes prior to analysis (C. Chen et al., 2022). The water repellency index is calculated as the ratio of the ethanol sorptivity to water sorptivity, which was determined in accordance with Lichner et al. (2012). The saturated water content was measured by oven drying method after fully saturating the samples, and the field capacity was determined by pressure plate apparatus at −33.0 kPa of soil water potential (S. L. Li et al., 2022b).

2.4. Measurements of Soil Vapor Diffusion

Soil vapor diffusion was measured by the gradient method (Luo & Tu, 2019). The soil sample collected in stainless steel cylinders was sealed on top of a glass beaker (6.5 cm diameter, 8.8 cm height) filled with distilled water (Figure 1h). As such, the RH inside the beaker (designated as RH_1) was maintained at 100%. Then, the sample and attached beaker were placed in an artificial climate incubator (Figure 1i; BIC-400, BOXUN Instrument, China), which provided a constant ambient RH (designated as RH_2) and temperature. As a result, the RH differential between RH_1 and RH_2 is the main factor driving vapor diffusion from the beaker through the soil sample and into the artificial climate incubator, which led to a mass loss from the beaker over time. Prior to the vapor diffusion measurement, the beaker was filled with 100 mL of distilled water, and soil samples were air-dried at temperature and RH of 20°C and 30%, respectively. During the measurement, the beaker and sample were taken out of the artificial climate incubator and weighed every 12 hr on a balance with a resolution of 0.01 g, and continuously measured for ∼5 days. The RH and temperature conditions of the artificial climate incubator were verified through a thermo-hygrometer. In this way, a series of ambient conditions were considered, which included temperature ranging from 20 to 50°C (with temperature increments of 10°C) at 50% RH, as well as, RH ranging from 30% to 70% (with RH increments of 20%) at 20°C.

The vapor diffusion flux and diffusivity were calculated using Equations 1 and 2 based on Fick's law (Fick, 1855):

$$J = \frac{1}{A}\frac{\mathrm{d}M}{\mathrm{d}t} \tag{1}$$

$$D = -J\frac{hRT}{P_0 m_0}\frac{1}{\Delta RH} \tag{2}$$

where J is the soil vapor diffusion flux (g cm^{-2} hr^{-1}); A is the cross-sectional area of the soil sample (cm^2); M is the mass of the water in the beaker (g); t is time (hr); D is the soil vapor diffusivity (cm^2 hr^{-1}); h is the height of the soil sample (cm); R is the universal gas constant (J K^{-1} mol^{-1}), which is 8.314 J K^{-1} mol^{-1}; T is the Kelvin temperature (K); P_0 is the saturated water vapor pressure (Pa); m_0 is the molar mass of water vapor (g mol^{-1}), which is 18.015 g mol^{-1}; and ΔRH is the difference between RH_1 and RH_2.

2.5. Measurements of Soil Vapor Adsorption

All the soil samples were air-dried at temperature and RH of 20°C and 30%, respectively, prior to the start of measurement. Vapor adsorption analysis of air-dried soil samples was also conducted using the artificial climate incubator. During the experiment, four levels of ambient temperatures (20, 30, 40, and 50°C) were considered at 50% of RH. Similarity, three levels of ambient RH (50%, 70%, and 90%) were selected at 20°C. The soil samples were weighed using a balance with 0.001 g resolution placed inside the incubator, and the weight was recorded at different time intervals throughout the measurements that lasted about 72 hr. The recorded time interval was shorter at the beginning of the experiment due to the initial rapid changes in the soil vapor adsorption rate, and the recorded time interval increased over time as the vapor adsorption gradually approached equilibrium and vapor adsorption rate approached zero. Once the soil sample weight increases per time interval remained constant for five consecutive intervals, we assumed that adsorption rate went to zero and cumulative vapor adsorption amount had reached its maximum. The initial vapor adsorption rate was calculated as the mean value of the first 2 hr. In this study, the vapor adsorption rate is defined as the net amount of water that is adsorbed per unit of time, and calculated as follows:

$$W = \frac{10\Delta m}{\rho\pi r^2 \Delta t} \tag{3}$$

where W is the vapor adsorption rate (mm hr^{-1}); 10 is the conversion factor used to convert cm hr^{-1} to mm hr^{-1}; Δm is the increase weight of the soil sample measured every interval (g); Δt is the time interval of the measurement (hr); ρ is the density of water (g cm^{-3}), which is 1.0 g cm^{-3}; r is the inner radius of the soil sample (cm).

2.6. Measurements of Soil Water Evaporation

The simulated evaporation experiment was conducted by using intact samples collected in the steel cylinders, similar to our previous studies (S. L. Li et al., 2022b). All samples were brought to the laboratory and saturated with water for 48 hr, and then they were covered by plastic films while allowing excess water to drain. Thereafter, the soil samples were gradually dried in the artificial climate incubator at six simulated atmospheric conditions (i.e., 20°C + 50% RH; 30°C + 50% RH; 40°C + 50% RH; 50°C + 50% RH; 20°C + 30% RH; and 20°C + 70% RH). During the experiments, all soil samples were weighed at constant time intervals with a balance (±0.001 g) to obtain the hourly evaporation amount, and measurements lasted 72 hr in total. The soil evaporation rate changes rapidly during the first few hours and then gradually becomes stable thereafter. Thus, all soil samples were weighed at 1 hr intervals for the first 4 hr and then weighed at about 12 hr intervals thereafter. The evaporation rate and cumulative evaporation amount were calculated according to S. L. Li and Xiao (2022):

$$E = \frac{10\Delta m}{\rho\pi r^2 \Delta t} \tag{4}$$

where E is the water evaporation rate (mm hr^{-1}); 10 is the conversion factor used to convert cm hr^{-1} to mm hr^{-1}; Δm is the change in weight of the soil sample (g) measured every time interval Δt (hr); ρ is the density of water (g cm^{-3}), which is 1.0 g cm^{-3}; r is the inner radius of the soil sample (cm).

In this study, the soil water evaporation was analyzed and expressed by the following three parameters: (a) initial stage evaporation rate (mm hr^{-1}), which was obtained from the average of evaporation rate within the first 12 hr; (b) late-stage evaporation rate (mm hr^{-1}), which was obtained from the average of evaporation rate within 12–72 hr; and (c) cumulative evaporation amount (mm), which was obtained from the total of evaporation amount within 72 hr.

2.7. Data Analysis

After normality and equality of variance tests, a one-way ANOVA with a least significant different post hoc test at 5% probability level was performed to investigate the differences in measured soil physicochemical properties, vapor diffusion and adsorption parameters, and water evaporation properties among the bare soil and three types of biocrusts. The final results represent the mean values of all replicates and are expressed as the mean ± standard error.

Pearson correlation analysis was applied to investigate the relationships between soil physicochemical properties, vapor diffusion properties, vapor adsorption capacity, and evaporation rate. Based on the Pearson correlation coefficients, we selected the main impact factors ($P < 0.05$) to establish structural equation models for testing the causal relationships between surface cover, soil physicochemical properties, vapor diffusion properties, vapor adsorption capacity, evaporation rate, RH, and temperature. To evaluate our hypothesis that biocrusts significantly alter soil properties and as a consequence soil water flux, we determined the absolute fit of the best models via the maximum likelihood χ^2/df, goodness of fit index (GFI), root mean square error of approximation, and P index.

3. Results

3.1. Biocrust Effects on Soil Vapor Diffusion

During the whole experiment, the cumulative vapor diffusion amount of all treatments increased linearly with time, and followed the ranked order of moss crusts > mixed crusts > cyano crusts > bare soil (Figure 2 and Figure S2 in Supporting Information S1). As shown in Table 1 and Table S1 in Supporting Information S1, the vapor diffusion properties (vapor diffusion flux and diffusivity) of the three types of biocrusts were significantly higher than those of the bare soil under the same ambient condition. Specifically, at the 50% RH condition, the cyano, mixed, and moss crusts increased the vapor diffusion properties by 5%–14%, 11%–24%, and 21%–37%, respectively, as compared with bare soil under isothermal conditions. Figure 3 shows that vapor diffusion properties changed with different ambient conditions. Specifically, the vapor diffusion flux and diffusivity of the biocrusts and bare soil increased exponentially once the temperature increased from 20 to 50°C under RH of 50% (Figures 3a and 3b). For all treatments at 50°C, 50% RH condition, the vapor diffusion flux and diffusivity were increased by 593%–631% and 146%–155%, respectively, as compared to the 20°C, 50% RH condition (Table 1).

Similarly, the vapor diffusion properties of the biocrusts under different RH were also greater than those of the bare soil at 20°C (Figure S2 in Supporting Information S1). At a temperature of 20°C and RH of 30%–70%, the vapor diffusion properties of the cyano, mixed, and moss crusts were respectively 9%–11%, 22%–26%, and 34%–39% higher than those of the bare soil (Table S1 in Supporting Information S1). Moreover, for all treatments at 20°C conditions, it was found that vapor diffusion flux and diffusivity decrease linearly with the increase of RH (Figures 3c and 3d). Noteworthy, the effect of RH on vapor diffusivity was not significant across each soil treatment.

3.2. Biocrust Effects on Water Evaporation

As depicted in Figure 4 and Figure S3 in Supporting Information S1, the evaporation rate of all treatments was the highest on the first day (Stage I) and then decreased slightly and thereafter rapidly (Stage II) until reaching very low, stable values (Stage III). Biocrusts greatly increased the late-stage evaporation rate (Stages II-III) and cumulative evaporation amount when compared to the bare soil (Table 2 and Table S2 in Supporting Information S1). All the treatments entered stage III during the evaporation experiments except for the moss crust at a temperature of 20°C (Figure 4). Specifically, at the RH of 50%, the initial stage evaporation rate of three types of biocrusts was 11% lower than that of the bare soil (0.382 vs. 0.431 mm hr^{-1}); however, they markedly increased late-stage evaporation rate by 169% (0.087 vs. 0.032 mm hr^{-1}) on average compared with the bare soil under the

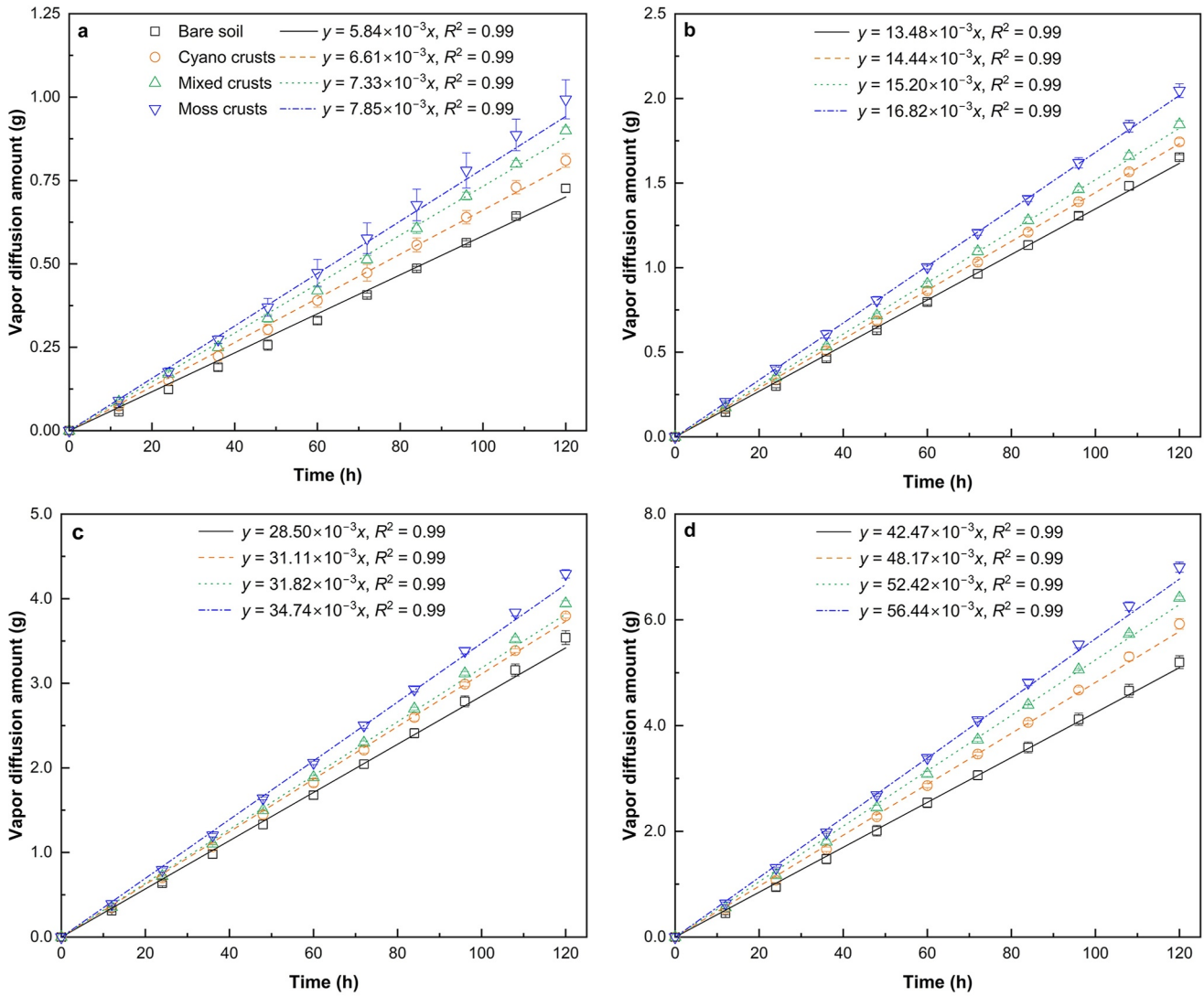

Figure 2. Cumulative water vapor diffusion curve of bare soil and three types of biocrusts under different temperature. (a) 20°C + 50% RH; (b) 30°C + 50% RH; (c) 40°C + 50% RH; and (d) 50°C + 50% RH.

temperature range of 20–50°C (Figure 4 and Table 2). In addition, at the 50% RH condition, the cumulative evaporation amount of all types of biocrusts were on average 38% (9.78 vs. 7.09 mm) higher in comparison to the bare soil, respectively (Figures 4 and 5). The greater effects on water evaporation process were from the moss crusts. For example, when the RH was 50%, the cumulative evaporation amount of moss crust (11.58 mm) was 42% and 20% higher than that of cyano (8.13 mm) and mixed crusts (9.64 mm), respectively. At a steady RH, the water evaporation rate and amount of all treatments increased with the increase in temperature (Figures 4 and 5). Particularly, the initial stage evaporation rate and cumulative evaporation amount of all types of biocrusts at 50°C was 0.507 mm hr^{-1} and 10.37 mm on average, which were 122% and 14% higher than those at 20°C (Table 2).

Although the water evaporation rate and amount under high RH (70%) of all treatments were significantly lower than those under lower RH (30% and 50%) at a steady temperature, the biocrusts still generated an increased effect of water evaporation rate and amount in contrast to bare soil under different RH conditions (Figures S3 and S4 in Supporting Information S1). Specifically, at 20°C, the late-stage evaporation rate of cyano, mixed, and moss crusts was 0.076, 0.106, and 0.140 mm hr^{-1}, exhibiting an increase of 35%, 88%, and 149%, respectively, as compared with bare soil (0.056 mm hr^{-1}) with the RH from 30% to 70% (Table S2 in Supporting Information S1). Correspondingly, the cumulative evaporation amount of cyano, mixed, and moss crusts was 10%, 34%, and 63% higher, respectively, than that of bare soil (Table S2 in Supporting Information S1). Furthermore, in comparison

Table 1
Water Vapor Diffusion Parameters of Bare Soil and Three Types of Biocrusts Under Different Temperature

Treatments	Ambient temperature (°C)	Ambient relative humidity (%)	Vapor diffusion flux ($\times 10^{-4}$ g cm^{-2} hr^{-1})	Vapor diffusivity (cm^2 hr^{-1})
Bare soil	20	50	1.01 ± 0.02 Dd	46.71 ± 0.74 Dd
	30	50	2.30 ± 0.02 Dc	60.54 ± 0.56 Dc
	40	50	4.92 ± 0.11 Db	77.01 ± 1.78 Db
	50	50	7.22 ± 0.17 Da	116.74 ± 2.72 Da
Cyano crusts	20	50	1.13 ± 0.03 Cd	52.06 ± 1.29 Cd
	30	50	2.42 ± 0.03 Cc	63.83 ± 0.76 Cc
	40	50	5.27 ± 0.03 Cb	82.59 ± 0.55 Cb
	50	50	8.23 ± 0.14 Ca	132.97 ± 2.25 Ca
Mixed crusts	20	50	1.25 ± 0.01 Bd	57.85 ± 0.64 Bd
	30	50	2.56 ± 0.03 Bc	67.62 ± 0.76 Bc
	40	50	5.48 ± 0.04 Bb	85.78 ± 0.70 Bb
	50	50	8.91 ± 0.04 Ba	144.05 ± 0.69 Ba
Moss crusts	20	50	1.38 ± 0.08 Ad	63.84 ± 3.77 Ad
	30	50	2.84 ± 0.06 Ac	74.94 ± 1.48 Ac
	40	50	5.96 ± 0.07 Ab	93.40 ± 1.07 Ab
	50	50	9.72 ± 0.13 Aa	157.07 ± 2.18 Aa

Note. Different uppercase letters (A–D) indicate significant differences ($\alpha = 0.05$) of water vapor diffusion parameters among different soil treatments of the same temperature. Different lowercase letters (a–d) indicate significant differences ($\alpha = 0.05$) of water vapor diffusion parameters among same soil treatments of the different temperature.

to the 30% RH condition, the late-stage evaporation rate and cumulative evaporation amount of the biocrusts were 6%–12% and 6%–11% lower at 70% RH condition (Figure S4 in Supporting Information S1).

3.3. Biocrust Effects on Soil Vapor Adsorption

As presented in Figure 6 and Figure S5 in Supporting Information S1, the vapor adsorption rate curves of the four treatments decreased sharply at first and then decreased slightly until approaching zero after the first few hours. From the initial to constant stages, the biocrusts showed much higher vapor adsorption rates (Figure 6 and Figure S5 in Supporting Information S1) and amounts (Figure 7 and Figure S6 in Supporting Information S1) than bare soil. Among the four treatments, the vapor adsorption capacity (initial vapor adsorption rate and total vapor adsorption amount) of the bare soil and moss crusts were the lowest and highest, respectively. As shown in Table 3, at RH of 50%, the initial vapor adsorption rate of cyano, mixed, and moss crusts were 0.047, 0.054, and 0.060 mm hr^{-1} on average at temperature of 20–50°C, respectively, which was 26%, 43%, and 59% higher, respectively, as compared to the bare soil (0.038 mm hr^{-1}). Correspondingly, the average total vapor adsorption amount of cyano, mixed, and moss crusts was significantly higher than that of bare soil (by 30%, 48%, and 65%, respectively; Table 3) with a temperature increase from 20 to 50°C. Furthermore, the temperature has a negative effect on the cumulative vapor adsorption amount. Specifically, for three types of biocrusts under 50% RH condition, the total vapor adsorption amount was 39%, 45%, and 52% lower at 30, 40, and 50°C in comparison to 20°C, respectively (Table 3).

However, at 20°C, the vapor adsorption capacity of all treatments increased with the increase of RH (Figures S5 and S6 in Supporting Information S1). As shown in Table S3 in Supporting Information S1, the biocrusts increased the initial vapor adsorption by 20%–41% for cyano crusts, by 34%–62% for mixed crusts, and by 43%–70% for moss crusts in comparison to bare soil with an increase in RH from 50% to 90%. Similarly, under full range of RH (50%–90%) at 20°C, the mean total vapor adsorption amount of cyano, mixed, and moss crusts was 38%, 60%, and 72% higher than at the bare soil, respectively (Table S3 in Supporting Information S1).

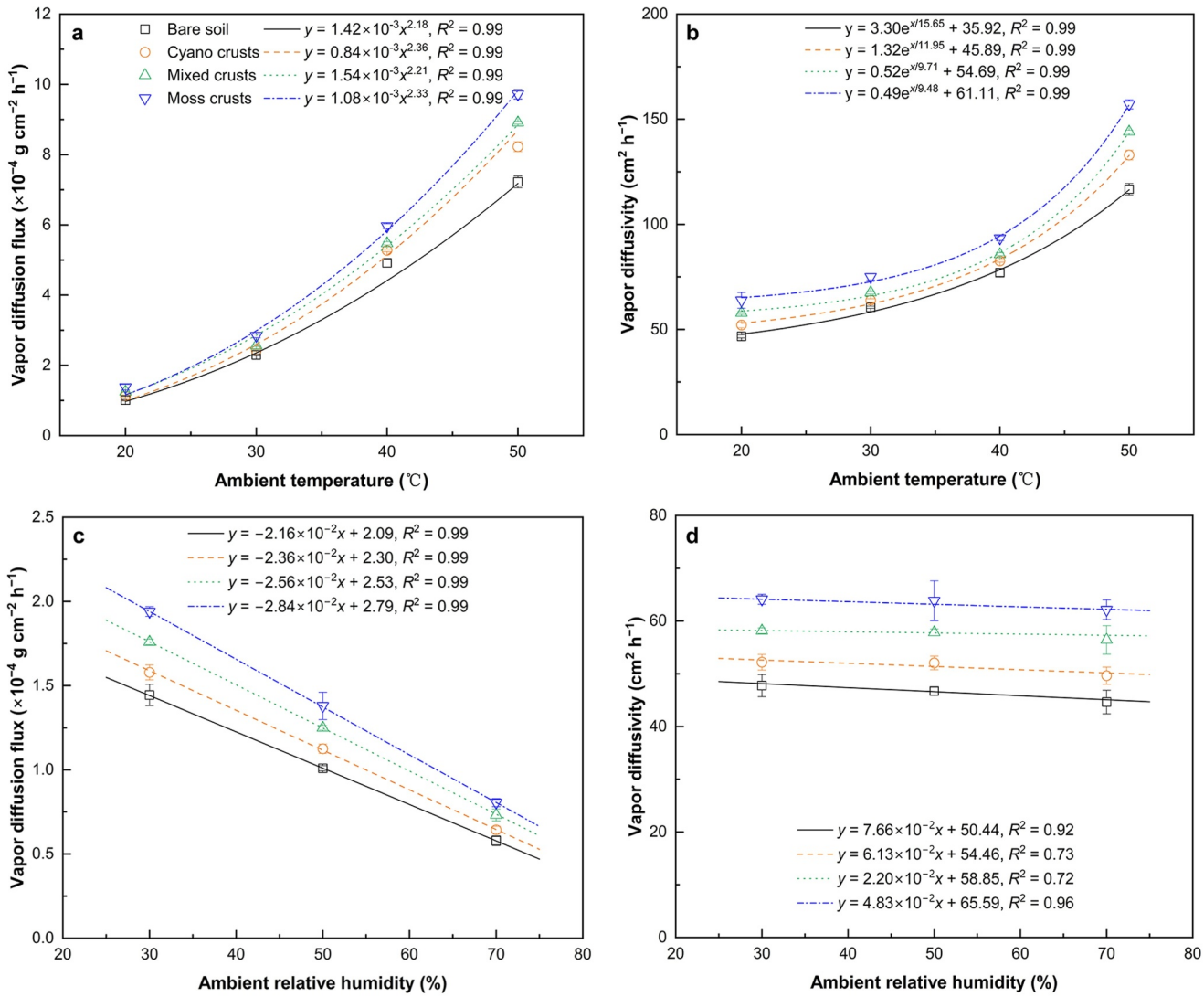

Figure 3. Water vapor diffusion flux and diffusivity with changing temperature (under 50% relative humidity condition; a and b) and relative humidity (under 20°C conditions; c and d) for bare soil and three types of biocrusts.

3.4. Effects of Soil Properties and Atmospheric Conditions on Soil Vapor Transport Properties

As shown in Table 4, biocrusts significantly changed all physiochemical properties compared to bare soil, and this was especially true for the moss crusts. All types of biocrusts had a much lower bulk density, but greater total porosity, fine particles (clay and silt) content, organic matter content, and specific surface area as compared with bare soil. Specifically, cyano, mixed, and moss crusts significantly decreased the bulk density (by 6%, 12%, and 32%, respectively) as compared to the bare soil. The total porosity, clay content, organic matter content, specific surface area, and water repellency index of biocrusts were 9%–50%, 9–37-fold, 161%–371%, 45%–90%, and 19%–91% higher than that of bare soil, respectively. The biocrusts also highly increased soil water holding capacity. All the cyano, mixed, and moss crusts had higher saturated water content (by 9%, 23%, and 66%, respectively) and field capacity (by 75%, 157%, and 251%, respectively) than the bare soil.

The vapor diffusivity, evaporation rate, and vapor adsorption amount were well correlated to other soil properties ($|r| \geq 0.81$; Figure 8). The vapor diffusivity, evaporation rate, and vapor adsorption amount showed high positive correlations with the clay content, organic matter content, specific surface area, and saturated water content ($P < 0.01$). Besides the soil properties, the total biomass and biocrust thickness were strongly positively correlated with vapor transport, which implied that the biological components in biocrusts (i.e., cyanobacteria and moss) can

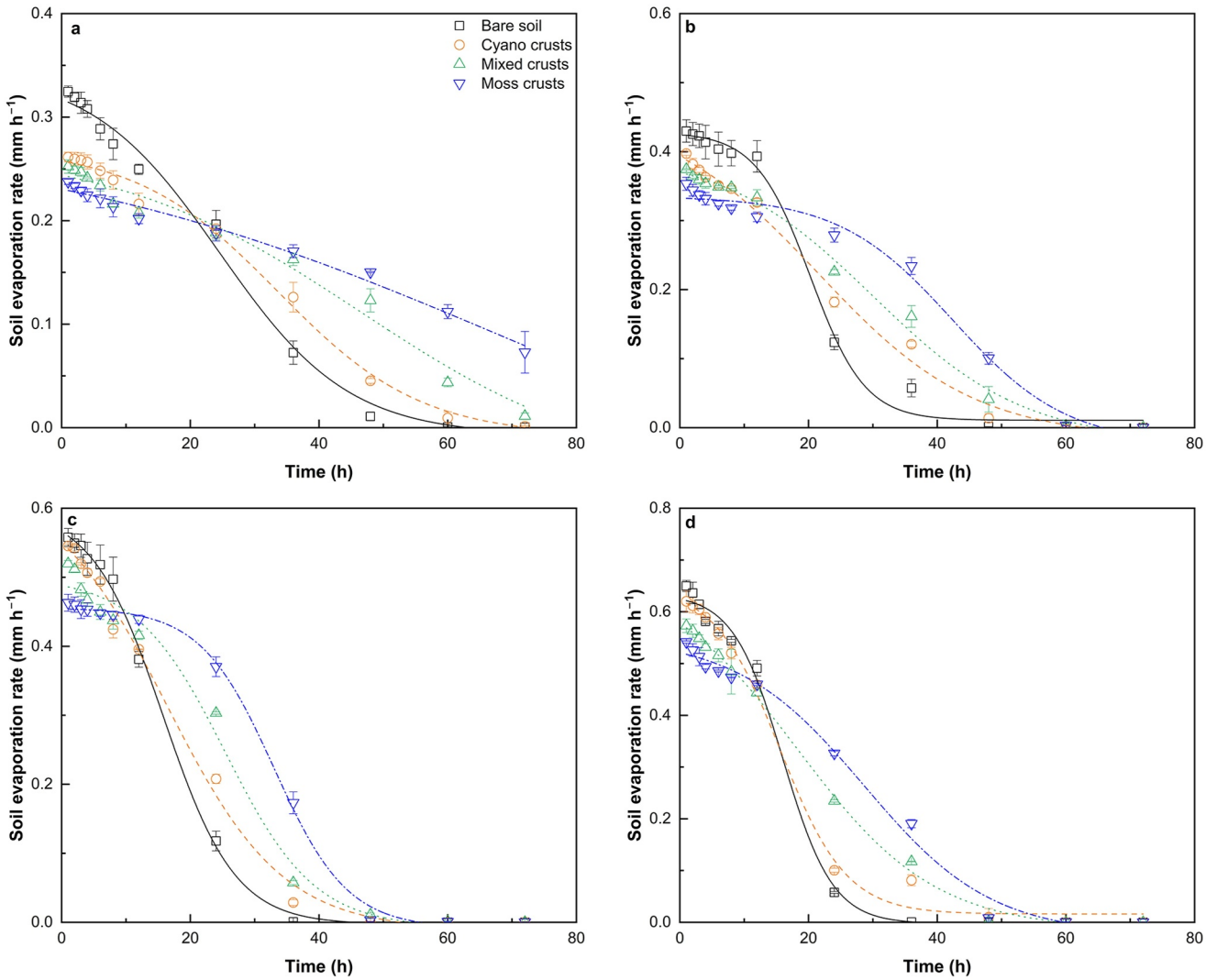

Figure 4. Soil evaporation rate of bare soil and three types of biocrusts under different temperature. (a) 20°C + 50% RH; (b) 30°C + 50% RH; (c) 40°C + 50% RH; and (d) 50°C + 50% RH.

have a strong influence on vapor flux. The structural equation model demonstrated that the surface cover has a significant direct impact on clay content, bulk density, specific surface area, and saturated water content ($|r| \geq 0.99$, $P < 0.05$; Figure S7 in Supporting Information S1). The biocrust cover indirectly affected soil vapor transport properties (i.e., vapor diffusion properties, vapor adsorption capacity, and water evaporation rate) via influencing soil physicochemical properties (i.e., bulk density, specific surface area, and saturated water content). Specifically, the bulk density negatively affected the soil vapor diffusion properties, which indicates that higher soil porosity facilitates the vapor flow. The specific surface area is positively correlated with vapor adsorption capacity, which suggests that a larger surface area increases the adsorption sites for water molecules. Furthermore, the clay content had a significant direct positive impact on water evaporation and also indirectly affected water evaporation through its influence on saturated water content.

In addition, the atmospheric conditions had significant direct effects on soil vapor transport properties (Figure S7 in Supporting Information S1). The ambient temperature was positively correlated with vapor diffusion properties and water evaporation, but negatively correlated with vapor adsorption capacity. Conversely, the ambient RH was negatively correlated with vapor diffusion properties and water evaporation, but positively correlated with vapor adsorption capacity. The structural equation model elucidated 87%–97% of the variance in the vapor transport.

Table 2
Water Evaporation Parameters of Bare Soil and Three Types of Biocrusts Under Different Temperature

Treatments	Ambient temperature (°C)	Ambient relative humidity (%)	Initial stage evaporation rate (mm hr^{-1})	Late-stage evaporation rate (mm hr^{-1})	Cumulative evaporation amount (mm)
Bare soil	20	50	0.283 ± 0.005 Ad	0.056 ± 0.003 Da	6.763 ± 0.125 Dc
	30	50	0.406 ± 0.021 Ac	0.037 ± 0.004 Db	7.063 ± 0.004 Db
	40	50	0.478 ± 0.015 Ab	0.024 ± 0.003 Dc	7.166 ± 0.054 Db
	50	50	0.556 ± 0.002 Aa	0.012 ± 0.000 Dd	7.374 ± 0.020 Da
Cyano crusts	20	50	0.240 ± 0.007 Bd	0.075 ± 0.002 Ca	7.367 ± 0.041 Cd
	30	50	0.351 ± 0.003 Bc	0.064 ± 0.001 Cb	8.042 ± 0.073 Cc
	40	50	0.461 ± 0.002 Bb	0.048 ± 0.001 Cc	8.395 ± 0.055 Cb
	50	50	0.535 ± 0.009 Ba	0.038 ± 0.002 Cd	8.722 ± 0.039 Ca
Mixed crusts	20	50	0.227 ± 0.003 Cd	0.106 ± 0.002 Ba	9.065 ± 0.059 Bd
	30	50	0.348 ± 0.005 Bc	0.086 ± 0.000 Bb	9.353 ± 0.085 Bc
	40	50	0.452 ± 0.004 Bb	0.075 ± 0.000 Bc	9.901 ± 0.029 Bb
	50	50	0.499 ± 0.011 Ca	0.071 ± 0.001 Bd	10.246 ± 0.111 Ba
Moss crusts	20	50	0.217 ± 0.002 Dd	0.139 ± 0.001 Aa	10.923 ± 0.039 Ad
	30	50	0.323 ± 0.002 Cc	0.123 ± 0.003 Ab	11.283 ± 0.160 Ac
	40	50	0.448 ± 0.007 Bb	0.110 ± 0.000 Ac	11.951 ± 0.024 Ab
	50	50	0.486 ± 0.004 Ca	0.105 ± 0.001 Ad	12.146 ± 0.013 Aa

Note. Different uppercase letters (A–D) indicate significant differences ($\alpha = 0.05$) of water evaporation parameters among different soil treatments of the same temperature. Different lowercase letters (a–d) indicate significant differences ($\alpha = 0.05$) of water evaporation parameters among same soil treatments of the different temperature.

4. Discussion

4.1. Biocrust Effects on Soil Vapor Diffusion and Their Underlying Mechanisms

Although only occupying a small portion of the soil profile, biocrusts are important biotic communities that regulate soil water transport in dryland ecosystems (Kidron, Fischer, & Xiao, 2022; S. L. Li, Bowker, & Xiao, 2021; Sun, Xiao, & Kidron, 2022). Vapor transport through the soil is mainly determined by the soil structure, especially water molecule diffusion paths within the soil (Luo & Tu, 2019). Overall, we found that biocrusts had a much higher soil vapor diffusion flux and vapor diffusivity than bare soil (Table 1 and Table S1 in Supporting Information S1), and these increased trends were mainly attributed to the modification of soil physicochemical properties induced by biocrusts, such as the lower bulk density and higher organic matter content (Table 4). Normally, the bulk density is an important indicator of the extent to which a soil has become compacted. In comparison to intact soil, compacted soil has higher bulk density and lower total porosity and macroporosity (Zhai & Horn, 2018). Alternately, the slight reduction in bulk density caused by biocrusts leads to a relative increase of pore space, thus increasing the pathways for vapor diffusion (Sun, Xiao, Kidron, & Markus, 2023). This result was also confirmed by the structural equation model analysis, which indicated that biocrusts significantly and indirectly affect soil gas diffusion properties through their influence on bulk density (Figure S7 in Supporting Information S1).

Biocrusts also facilitate soil aggregation and aggregate stability through their provision of cementing substances (i.e., organic matter and clay), thus increasing soil porosity and vapor diffusion rate (Peng et al., 2022). Moreover, the organic matter can cohere mineral particles, thereby effectively promoting soil structural pore formation, expanding pore size, and altering pore connectivity (Sun, Xiao, Li, et al., 2023). In this study, the organic matter content and clay content of biocrusts were 161%–371% and 9–37-fold higher than those of the bare soil, respectively, especially for the moss crusts (Table 4). Apart from the soil properties, the biotic components of biocrusts, such as filamentous biological components (e.g., moss rhizoids, lichen rhizines, and cyanobacterial filaments), microscopic fungal hyphae, and polysaccharide and organic gels secreted by cyanobacteria, could also combine the microaggregates further to form macroaggregates and generate more pores in microaggregates (Weber et al., 2022; Zhang et al., 2006). Moreover, the exopolysaccharides secreted by biocrusts can act as gluing

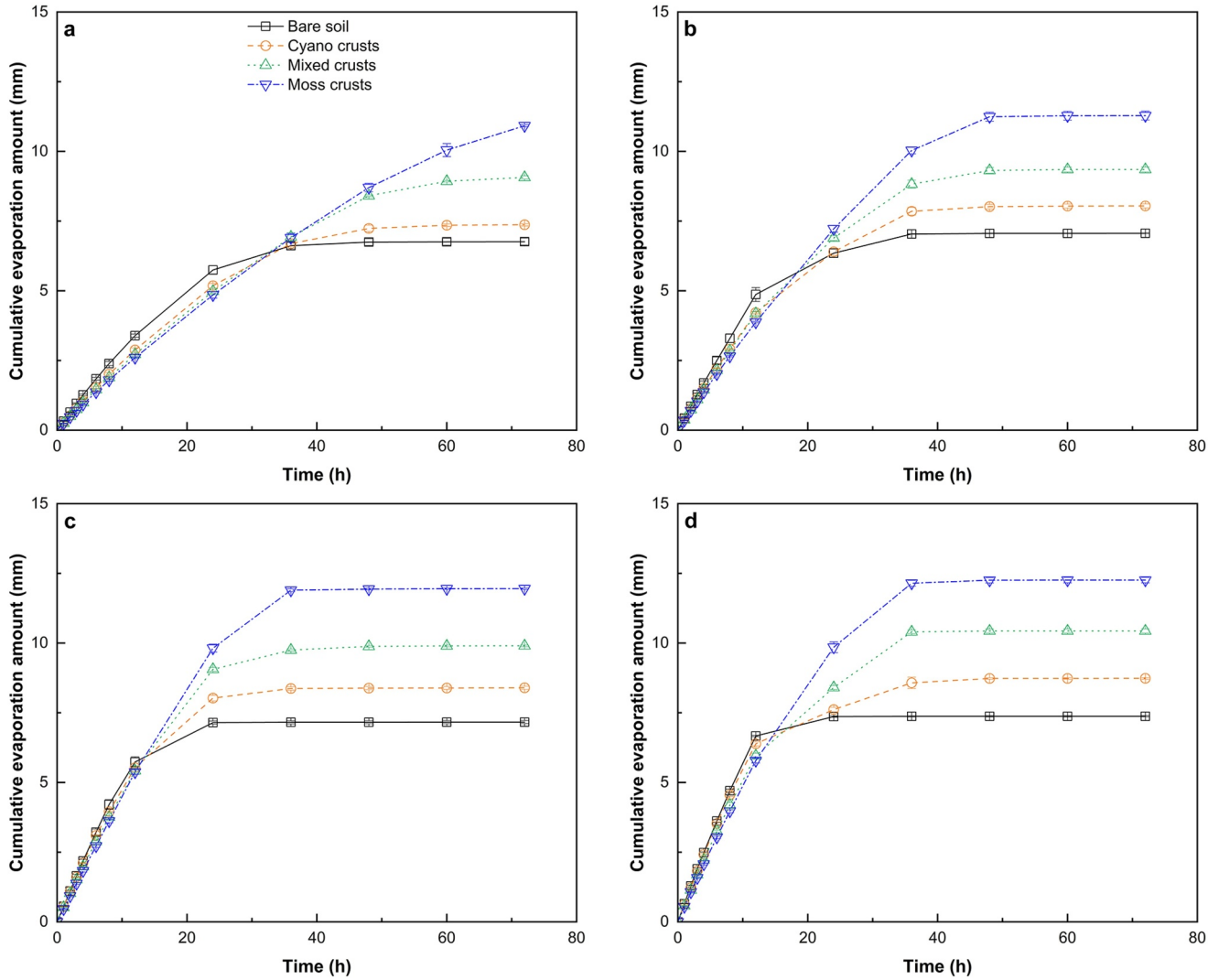

Figure 5. Cumulative evaporation curve of bare soil and three types of biocrusts under different temperature. (a) 20°C + 50% RH; (b) 30°C + 50% RH; (c) 40°C + 50% RH; and (d) 50°C + 50% RH.

agents, and contribute directly to aggregate stability (Chock et al., 2019; Xiao, Sun, Hu, & Kidron, 2019). Furthermore, soil pore morphology plays a crucial role in vapor and gas transmission (Peng et al., 2022; Sun, Xiao, Kidron, & Heitman, 2022). In a porous media, the vapor mainly diffuses through connected pores. In the same study area, the pore structure of biocrusts obtained by analyzing X-ray CT images showed that biocrusts increased the macroporosity and pore size volume in contrast to bare soil, and the fraction of large, long-shaped, and continuous pores accounted for 81%–96% of the total pore volume in the biocrusts (Sun, Xiao, Li, et al., 2023). Similar results are reported by Menon et al. (2011) and Xiao, Sun, Hu, and Kidron (2019), who pointed out that the colonization of biocrusts is positively correlated with soil porosity and pore structure. Additionally, the root-like structures (i.e., lichen rhizines, moss rhizoids, and protonemata) and enhanced activity of microbial and soil fauna communities in biocrusts may also be beneficial to generate biopores with long and continuous pore shapes (L. C. Liu et al., 2017; Souza-Egipsy et al., 2004), which is important for water vapor transport. Consequently, an increase in the soil porosity and organic matter content, as well as the continuous pore structure in biocrusts contributed to the increase in soil vapor diffusion properties.

The modification of bulk density may be attributed to the increase in organic matter and fines content. Whereas organic carbon fixation by the photoautotrophic component of the biocrusts (cyanobacteria, lichens, and mosses) is mainly responsible for the increase in organic matter of the crust (Beymer & Klopatek, 1991; Lange

10.1029/2023WR036520

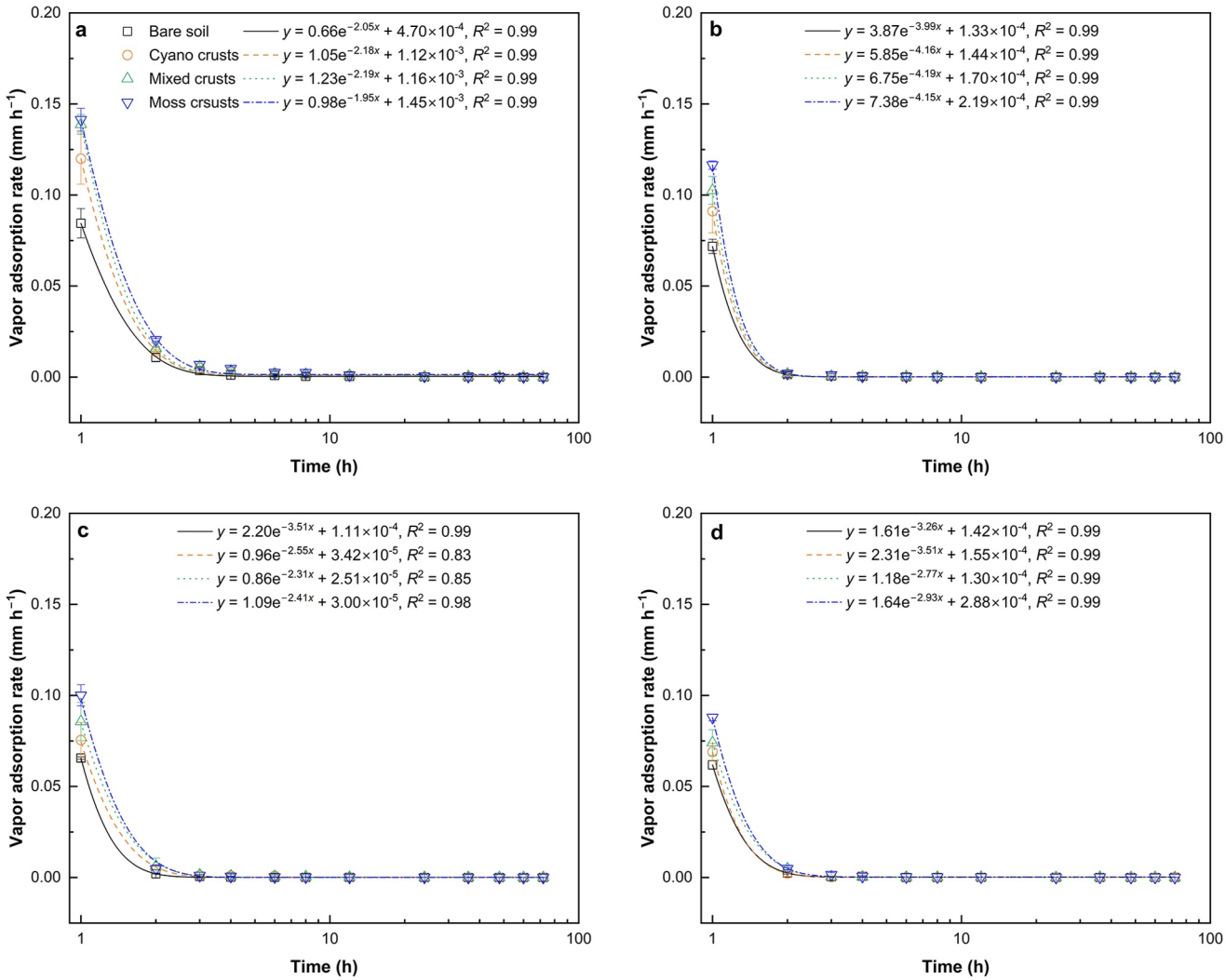

Figure 6. Water vapor adsorption rate of bare soil and three types of biocrusts under different temperature. (a) 20°C + 50% RH; (b) 30°C + 50% RH; (c) 40°C + 50% RH; and (d) 50°C + 50% RH.

et al., 1992), dust entrapment (Danin & Ganor, 1991), as well as bioweathering by the crusts (R. Y. Chen et al., 2009) promote the formation of fine particles. Biocrusts may also increase the soil carbon pool by secreting extracellular polymeric substances (EPS) (Mager & Thomas, 2011). All the above will result in a decrease in bulk density and an increase in soil porosity, which point to a better structure than the bare soil, in turn, affecting the vapor diffusion properties.

Apart from the soil properties, it has been suggested that atmospheric conditions are the major driving force for soil vapor diffusion (Luo et al., 2018). In our study, at a given temperature, the vapor passes through the soil sample driven by the RH gradient between the environmental chamber and the solution container (which is filled with distilled water). In general, the vapor moves through soil sample in response to concentration gradients, therefore, the RH gradient is positively correlated with the soil vapor diffusion rate (Jabro, 2009). In addition, the maximum values of soil vapor diffusivity are always reached at the maximum ambient temperature of all treatments, suggesting that soil vapor diffusion may be enhanced from an increase in ambient temperature (Table 1). In comparison to the RH gradients, the temperature gradient had a significant effect on soil vapor diffusivity (Table 1 and Table S1 in Supporting Information S1). This is attributed to an increase in the kinetic energy of the water molecules with the increase in ambient temperature, which in turn increases their velocity while diffusing and may also reduce the duration of time that they are adsorbed along the pathway.

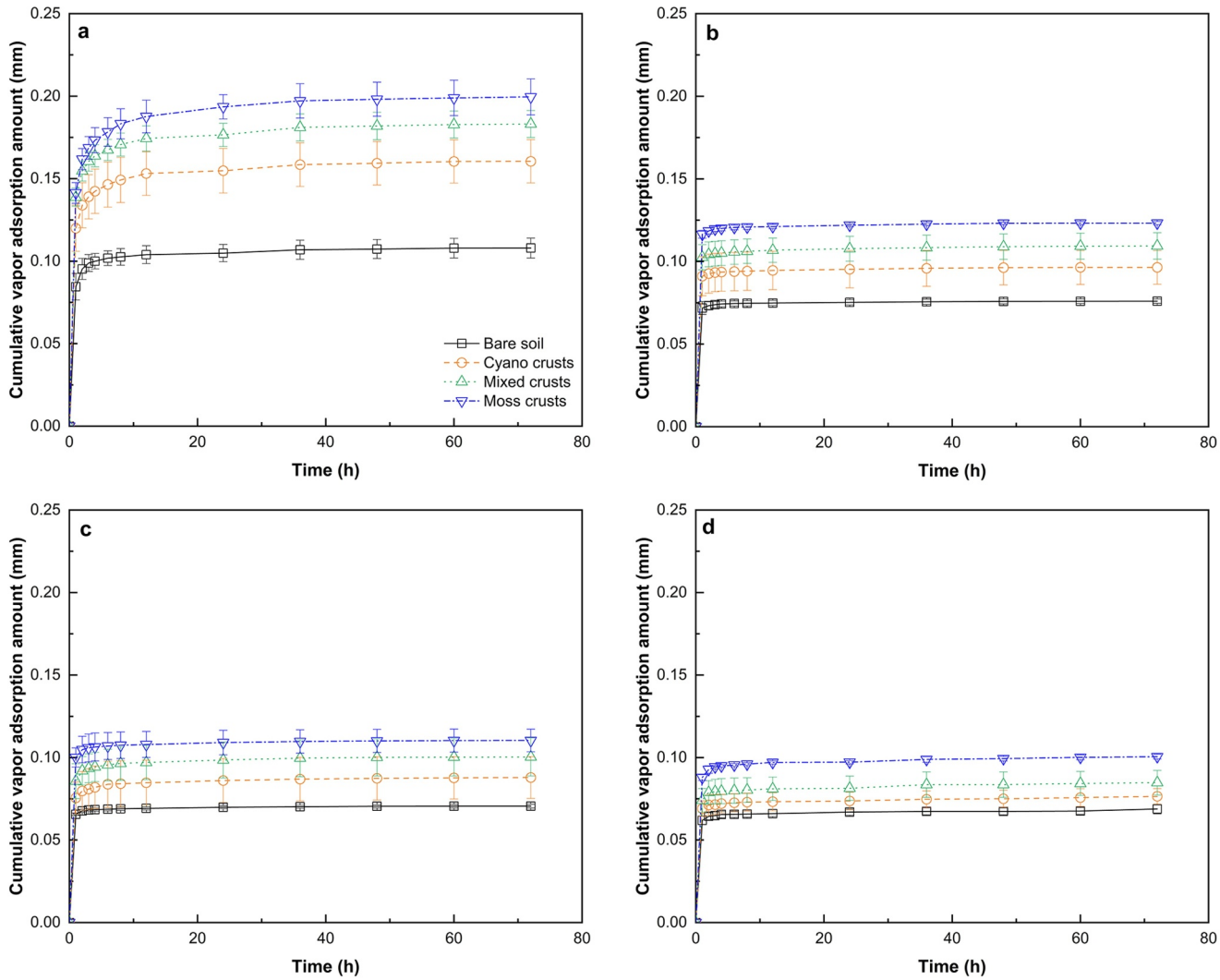

Figure 7. Cumulative water vapor adsorption curve of bare soil and three types of biocrusts under different temperature. (a) 20°C + 50% RH; (b) 30°C + 50% RH; (c) 40°C + 50% RH; and (d) 50°C + 50% RH.

In our study, for a temperature rise from 20 to 50°C, the increase of vapor diffusivity of soil samples is higher than that of free air. The following two reasons may explain the increase of diffusion coefficient of biocrusts and bare soil. First, during the vapor diffusion experiment, vapor adsorption occurs simultaneously with vapor diffusion. Especially, the capillary condensation in the soil may impede the pathways for vapor transport during the vapor diffusion. As the temperature is increased, less vapor is adsorbed at a given RH by mineral surface due to molecules tending to desorb from the surface at elevated temperatures. Therefore, the pathway of vapor diffusion and water molecules kinetic energy increases with increasing temperature, thereby increasing the speed of water molecules to penetrate the soil sample. Second, the artificial climate incubator maintains a stable RH by adding water vapor. In order to maintain a constant RH in the artificial climate incubator at elevated temperatures, a large amount of water vapor needs to be introduced into the incubator, thereby increasing the air flow rate of the soil sample and facilitating vapor diffusion.

4.2. Underlying Mechanisms of Biocrust Affecting Soil Evaporation

Overall, we found that the average evaporation rate of all types of biocrusts was significantly higher than that of bare soil, indicating that the colonization of biocrusts could enhance soil evaporation in drylands (Table 2). We attributed the increasing effects of biocrusts on soil evaporation to biocrust-mediated changes in soil properties and hydraulic parameters (Kidron & Tal, 2012; X. R. Li et al., 2018; Xiao et al., 2010). Since the evaporation

Table 3
Water Vapor Adsorption Parameters of Bare Soil and Three Types of Biocrusts Under Different Temperature

Treatments	Ambient temperature (°C)	Ambient relative humidity (%)	Initial vapor adsorption rate (mm hr^{-1})	Initial vapor adsorption amount (mm)	Cumulative vapor adsorption amount (mm)
Bare soil	20	50	0.048 ± 0.003 Ca	0.095 ± 0.006 Ca	0.108 ± 0.006 Ca
	30	50	0.037 ± 0.001 Cb	0.073 ± 0.002 Cb	0.076 ± 0.001 Db
	40	50	0.034 ± 0.000 Cbc	0.068 ± 0.001 Cbc	0.071 ± 0.001 Cbc
	50	50	0.032 ± 0.001 Cc	0.064 ± 0.002 Cc	0.069 ± 0.003 Cc
Cyano crusts	20	50	0.067 ± 0.007 Ba	0.134 ± 0.014 Ba	0.161 ± 0.013 Ba
	30	50	0.046 ± 0.006 Bb	0.093 ± 0.012 Bb	0.096 ± 0.010 Cb
	40	50	0.040 ± 0.006 BCb	0.080 ± 0.012 BCb	0.088 ± 0.013 BCb
	50	50	0.036 ± 0.003 BCb	0.071 ± 0.006 BCb	0.076 ± 0.005 BCb
Mixed crusts	20	50	0.077 ± 0.003 Aa	0.155 ± 0.006 Aa	0.183 ± 0.008 Aa
	30	50	0.052 ± 0.004 Bb	0.104 ± 0.008 Bb	0.109 ± 0.008 Bb
	40	50	0.046 ± 0.004 ABbc	0.092 ± 0.009 ABbc	0.100 ± 0.012 ABbc
	50	50	0.039 ± 0.004 Bc	0.079 ± 0.007 Bc	0.085 ± 0.007 Bc
Moss crusts	20	50	0.081 ± 0.003 Aa	0.162 ± 0.006 Aa	0.200 ± 0.011 Aa
	30	50	0.059 ± 0.001 Ab	0.118 ± 0.002 Ab	0.123 ± 0.001 Ab
	40	50	0.052 ± 0.004 Ac	0.105 ± 0.008 Ac	0.110 ± 0.007 Ac
	50	50	0.046 ± 0.001 Ad	0.093 ± 0.002 Ad	0.101 ± 0.001 Ac

Note. Different uppercase letters (A–D) indicate significant differences ($\alpha = 0.05$) of water vapor adsorption parameters among different soil treatments of the same temperature. Different lowercase letters (a–d) indicate significant differences ($\alpha = 0.05$) of water vapor adsorption parameters among same soil treatments of the different temperature.

Table 4
Properties of Bare Soil and Three Types of Biocrusts

Measurements	Bare soil	Cyano crusts	Mixed crusts	Moss crusts	*F*	*P*
Total biomass (g cm^{-2})	–	0.07 ± 0.01 c	0.12 ± 0.01 b	0.17 ± 0.01 a	34.82	<0.001
Biocrust thickness (mm)	–	6.29 ± 0.39 c	8.64 ± 0.24 b	11.45 ± 0.47 a	137.96	<0.001
Chlorophyll *a* content (μg g^{-1})	–	5.76 ± 0.52 c	8.43 ± 0.30 b	10.13 ± 1.03 a	30.57	0.001
Crust coverage (%)	–	90.96 ± 1.82 c	94.83 ± 1.70 b	95.84 ± 2.15 a	5.50	0.044
Bulk density (g cm^{-3})	1.61 ± 0.01 a	1.51 ± 0.01 b	1.42 ± 0.02 c	1.09 ± 0.08 d	96.22	<0.001
Total porosity (%)	39.37 ± 0.56 d	42.99 ± 0.48 c	46.40 ± 0.69 b	59.01 ± 2.89 a	84.85	<0.001
Sand content (20–2,000 μm) (%)	97.77 ± 0.12 a	88.96 ± 0.18 b	84.29 ± 0.16 c	78.88 ± 0.43 d	2938.15	<0.001
Silt content (2–20 μm) (%)	2.21 ± 0.12 d	10.83 ± 0.18 c	15.28 ± 0.17 b	20.32 ± 0.40 a	3031.93	<0.001
Clay content (<2 μm) (%)	0.02 ± 0.00 d	0.21 ± 0.01 c	0.43 ± 0.01 b	0.80 ± 0.04 a	835.52	<0.001
Organic matter content (g kg^{-1})	6.42 ± 0.68 d	16.74 ± 0.99 c	25.38 ± 0.62 b	30.36 ± 0.34 a	685.59	<0.001
Soil pH	8.21 ± 0.01 a	7.65 ± 0.01 b	7.63 ± 0.01 b	7.49 ± 0.08 c	170.19	<0.001
Specific surface area (m^2 g^{-1})	1.55 ± 0.15 d	2.25 ± 0.04 c	2.52 ± 0.06 b	2.95 ± 0.10 a	112.13	<0.001
Water drop penetration time (s)	1.51 ± 0.52 a	1.70 ± 0.42 a	1.72 ± 0.16 a	1.80 ± 0.27 a	0.564	0.647
Water repellency index	2.19 ± 0.18 d	2.60 ± 0.05 c	3.57 ± 0.10 b	4.18 ± 0.18 a	281.97	<0.001
Saturated water content (cm^3 cm^{-3})	0.34 ± 0.02 d	0.37 ± 0.01 c	0.42 ± 0.01 b	0.56 ± 0.02 a	32.74	<0.001
Field capacity (cm^3 cm^{-3})	0.05 ± 0.01 d	0.09 ± 0.01 c	0.14 ± 0.01 b	0.18 ± 0.03 a	117.60	<0.001
Surface roughness (%)	2.56 ± 0.26 d	8.55 ± 0.39 c	16.58 ± 1.16 a	12.22 ± 0.82 b	189.08	<0.001

Note. Different lowercase letters (a–d) within the same row indicate significant differences ($\alpha = 0.05$) among soil treatments.

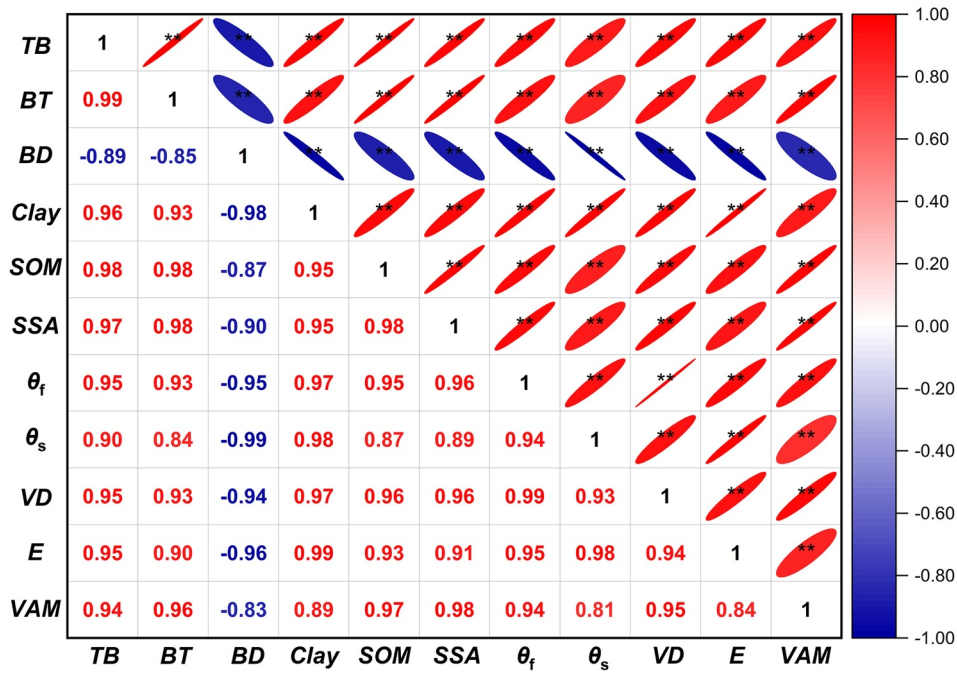

Figure 8. Pearson correlation coefficients matrix for total biomass (*TB*), biocrust thickness (*BT*), soil bulk density (*BD*), clay content (*Clay*), soil organic matter content (*SOM*), specific surface area (*SSA*), field capacity (θ_f), saturated water content (θ_s), vapor diffusivity (*VD*), evaporation rate (*E*), and vapor adsorption amount (*VAM*). The correlation coefficients are listed in the lower left of matrix and the significance is presented in the upper right matrix. The red color indicates positive correlations, and the blue color indicates negative correlations. * and ** indicate that the coefficients are significant at the 0.05 and 0.01 probability levels, respectively.

process can be divided into three stages (Lal & Shukla, 2004), it is noteworthy that biocrusts decreased the rate of water evaporation at stage I but increased at stages II–III (Figure 4 and Figure S3 in Supporting Information S1). At the initial stage, all treatments had high soil water content (near saturated water content) in our study, and the evaporation rate was the highest while being limited by atmospheric condition (S. L. Li et al., 2022b). The decreased initial evaporation rate of biocrusts can be explained by the high absorption capability of the biocrust, mainly induced by their high EPS (Chock et al., 2019; Lan et al., 2012). Secreted by cyanobacteria, microalgae, microfungi, and bacteria (Kidron et al., 2020; Rossi et al., 2012), the EPS are an essential component of the surface soil matrix structure and of biocrust function. Upon wetting, EPS was reported to expand its volume within seconds (up to 70-fold its dry weight; Chenu, 1993), thereby increasing its water-holding capacity and leading to surface sealing and pore clogging. As noted by Kidron et al. (2020), a large amount of loosely-bound EPS can be noted by SEM pictographs, and these scattered EPS may inevitably lead to the reduction in available pore space near the soil surface. Moreover, upon wetting, the cyanobacterial sheath swells and becomes turgid, subsequently restricting the pathways for vapor transport during the initial stage of evaporation (Fischer et al., 2010; Verrecchia et al., 1995). The formation of a dry layer during the later stages of evaporation may retard vapor transport and subsequently evaporation, as shown during later times (i.e., hours 24–72). Biocrusts could maintain more water and delay the formation of a dry surface layer (S. L. Li & Xiao, 2022). The enhanced pore connectivity and reduced tortuosity in biocrusts contribute to a decrease in diffusive length (Sun, Xiao, Li, et al., 2023), facilitating the transport of moisture toward the evaporation front and shortening the time required for water vapor in the drying surface layer to escape into the atmosphere. In contrast to vascular plants, mosses are poikilohydric and lack both a typical vascular conducting system for water and stomatal pores for control of transpiration, and therefore, mosses are thought to evaporate freely (Merced & Renzaglia, 2017). Consequently, biocrusts promote soil evaporation rate during the later stages of the evaporation process. Similar results of biocrusts' impact on water evaporation were also reached by S. L. Li et al. (2022a, 2022b), maintaining that the biocrusts could decrease the water evaporation rate at stage I, but increase water evaporation rate and water loss during stages II and III.

In the late stages of evaporation, the water migrates in the form of vapor diffusion, and from the subsurface soil toward ambient atmosphere. Both the soil evaporation and vapor diffusion involve the vertical transport of water through the soil. However, there are some differences between the late-stages evaporation and vapor diffusion. First, as evaporation goes on, the evaporation front moves continuously downwards, and thus the temperature at the soil surface is higher than that at the bottom. In our study, at the late stages of evaporation, the thermal and concentration gradients are the driving forces for vapor diffusion. During the vapor diffusion experiment, the artificial climate incubator provided uniform heating conditions by transferring the heat to the test device for the water vapor measurements, and the concentration gradient provided the dominant driving force for the diffusion of water vapor. Second, despite the fact that this study only measured vapor diffusion process in the surface soil, it can actually take place in the whole soil profile; however, late-stage evaporation process only occurs above the evaporation front. Third, the vapor diffusion coefficient cannot be obtained from the soil evaporation process, and the measurement of vapor diffusion is essential for further understanding the effects of biocrusts on evaporation process in the late stages.

It is well documented that atmospheric conditions (i.e., RH, temperature, radiation, and wind velocity) play significant roles in soil water evaporation (Smits et al., 2012), that is, vapor transport toward the atmosphere (de Amesti et al., 2020). Vapor transport from the soil toward the atmosphere occurs when the vapor pressure of the soil air is greater than the vapor pressure of the atmosphere during a continuous supply of evaporative energy and water (Lopez-Canfin et al., 2022). In our study, the evaporation rate of all treatments was negatively correlated with the ambient RH. The lower the ambient RH, the drier the air and the higher the differences in vapor pressure. On the other hand, higher temperatures positively affect the evaporation rate. As the ambient temperature increases, the amount of energy necessary for evaporation decreases. Noticeably, all three types of biocrusts had higher evaporation rates and amounts than bare soil under all atmospheric conditions considered in our study, which implies that the biocrust layer is important to mediating boundary conditions for water evaporation and balance in drylands.

4.3. Pathways of Biocrust Effects on Soil Vapor Adsorption

The capability of soils to adsorb vapor is dependent on various factors, such as soil properties, ambient temperature, and sorption direction. Our study showed that the biocrusts had higher vapor adsorption rate and amount than bare soil, which suggests that biocrusts improve vapor sorption capacity. Generally, the soil vapor sorption capacity increases with increasing soil clay content, specific surface area, and cation exchange capacity (C. Chen et al., 2021). The increased vapor sorption capacity of biocrust is modulated by the change in the soil particle size composition and specific surface area (Table 4). The interlayer swelling characteristics of clay minerals increase the surface area and adsorption sites, thereby facilitating the adsorption of a larger quantity of monolayer water and hygroscopic water than do sand grains (Schneider & Goss, 2012). The abundant fine particles (especially clay content) in biocrusts provide a greater quantity of adsorption sites for water molecules, therefore higher adsorption capacity of biocrusts, even when clay mineralogy in the biocrusts is similar to that of the bare soil (C. Chen et al., 2021). In addition, increased surface roughness also contributes to higher water molecule adsorption, as well as cation hydration (Arthur, 2017; Song et al., 2022). Specifically, during the monolayer adsorption stage, mineral soils adsorb water molecules through hydration (cation and surface hydration) (Khorshidi & Lu, 2017). As the clay particles have relatively large surface areas, they are the primary sites of cation retention and exchange in soils (C. Chen et al., 2021). Thus, biocrusts could also improve soil vapor adsorption through their higher cation exchange capacity and specific surface area (Kheirfam & Roohi, 2020). This finding was confirmed by the structural equation model, which showed that clay content and specific surface area are the key driving factors of soil vapor adsorption capacity. Similar results were also reported by S. L. Li, Xiao, et al. (2021) and Song et al. (2022), who documented that clay content is strongly correlated with specific surface area and water vapor sorption amount.

Organic matter also has a significant impact on vapor adsorption capacity, for it can coat the surface of clay minerals and increase the surface area accessible to water molecules (S. L. Li, Xiao, et al., 2021). Soil organic matter could directly adsorb water due to the presence of hydrophilic oxygen-containing functional groups, which included carboxylic, phenolic hydroxyl, and amino groups (Arthur et al., 2020; Kirschbaum et al., 2020). Accordingly, our biocrusts should have a higher vapor adsorption capacity because they generally have a higher organic matter content in comparison to the bare soil (Table 4). In our study, moss-inhabited biocrusts (moss and mixed crusts) could engineer more profound changes in the soil vapor adsorption capacity than cyano crusts and

bare soil (Table 3 and Table S3 in Supporting Information S1). With the successional transition from cyanobacterial to moss, biocrusts can engineer profound changes in the soil properties and further influence vapor adsorption capacity through several processes. Due to their greater surface roughness, biomass, and thickness, moss-inhabited biocrusts can fix greater amounts of carbon and trap higher amounts of fines, thereby generally enhancing all of the soil properties discussed above, such as clay content, specific surface area, and organic matter content (Karnieli et al., 1999), often more significantly than cyano crusts. Consequently, the biocrust layer could improve soil vapor adsorption, and the thicker the biocrust layer, the greater the improvement (S. L. Li, Bowker, & Xiao, 2021).

In addition to the soil properties, the biological components in biocrusts (i.e., cyanobacteria and moss) can have a strong influence on vapor adsorption. Soil bacteria directly influence water acquisition and retention through the secretion of EPS (Y. S. Guo et al., 2018). EPS are composed of compositionally heterogeneous high-molecular-weight glycan polymers rich in free hydroxyl (-OH) and amino ($-NH_2$) group, both of which are strongly hydrophilic and contribute to water uptake from the atmosphere and hold moisture directly within the EPS polymeric matrix (Wang et al., 2012). Moreover, EPS can act as binding agents for aggregates on micrometer scale (Godinho & Bhosle, 2009), and play a crucial role in maintaining structural stability (Flemming & Wingender, 2010). The small pores typical of intra-aggregate spaces hold water tightly, thereby modulating soil moisture (Lehmann et al., 2017). Although the mosses are small, they have papillae and lamellae on their costae, as well as moss cushions and the rhizoids (root-like structures) that anchor the plants to the ground, which can absorb water directly from the atmosphere (Kidron et al., 2002; Nejidat et al., 2016). Moreover, the biotic component could also exert an important effect on soil properties. Therefore, with succession from cyanobacterial to moss, a crucial functional change is also expected, which further strongly influences soil vapor adsorption capacity.

Soil water repellency also plays a crucial role in vapor sorption by influencing available sorption sites. Many scholars maintain that biocrusts are water repellent, mainly attributed to the organic matter and non-polar exudates of microorganisms (e.g., green algae or cyanobacteria), which could increase the contact angle of the water with the soil surface (Fischer et al., 2010). In this study, the water repellency was assessed by water drop penetration time and water repellency index. According to Bisdom et al. (1993), water drop penetration time less than 5 s implies non-repellent conditions. Although the biocrusts had higher water drop penetration time than bare soil, the average water drop penetration time of biocrusts was 1.74 s, which showed that they were non-repellent (Table 4). Unlike water repellency index >9, which implied hydrophobicity (Fischer et al., 2010), RI of up to 4–5 in our study did not necessarily indicate crust hydrophobicity. Additionally, no conclusive evidence has yet been reported showing runoff generation ascribed to water repellency in arid and semiarid regions (Kidron, 2019). While the biocrusts had higher water drop penetration time and repellency index than bare soil, the difference of soil properties (e.g., clay content, specific surface area, and organic matter content) and biological component played a leading role in vapor adsorption.

4.4. Implication for Biocrust Role in Soil Vapor Transport Related Dryland Ecohydrology

As an important living skin in drylands, biocrusts substantially regulate soil water transport, which means that they are essential agents in changing ecohydrological, biological, and chemical processes (Xiao et al., 2022). In this study, we found that biocrusts greatly enhanced soil vapor transport properties, and all these effects were reasonably attributed to the biocrusts' modifications on soil properties. Generally, water transport in relatively dry soils is not a simple vapor diffusion process. The diffusion of vapor is coupled with the exchange of water between liquid and vapor phases (evaporation and condensation), and the adsorption of water molecules on soil surfaces. These processes may occur simultaneously, and the net result of all processes was measured in the study. Due to strong evaporation and large temperature differences between day and night, liquid water and vapor transitions take place frequently in drylands. For example, following rain liquid water evaporates to form vapor, and subsequently the vapor condenses as liquid water on a cooler surface at night driven by the temperature gradient (Cahill & Parlange, 1998; Kidron, Kronenfeld, et al., 2022). Since the condensation capacity shows a positive correlation with the amount of adsorption sites for water molecules (C. Chen et al., 2021), biocrusts are expected to increase condensation capacity (e.g., vapor condensation and dew formation), which is confirmed by the finding of S. L. Li, Bowker, and Xiao (2021), who documented an increment in high daily non-rainfall water amount in biocrusts. Nevertheless, as found for the Negev, non-rainfall water had only a limited effect on biocrusts, explained by the substantially higher nocturnal temperatures of the surface (Kidron & Kronenfeld, 2023).

In the Negev, non-rainfall water was however shown to have a positive effect on moss crusts. Protruding several millimeters above the soil surface, mosses were found to experience efficient nocturnal cooling which facilitate in turn dew formation (Kidron et al., 2002).

It is well known that the vapor transport is coupled with heat transport, as large value of the latent energy is required for vapourization of water (Parlange et al., 1998). The biocrust influence on soil temperature can be better understood by assessing the effects of biocrusts on soil vapor transport. By increasing soil water holding capacity, vapor diffusivity, and evaporation rate, biocrusts facilitate vapor transport from soil to atmosphere after rainfall events, thus demanding more heat and energy for vapor to diffuse through the dry layer to the soil surface. Moreover, recent studies reported that biocrusts significantly increased heat capacity, thermal conductivity, and thermal diffusivity of surface soil by holding more water when wet (Xiao, Ma, & Hu, 2019), which will inevitably reduce the surface temperature (S. L. Li & Xiao, 2022; Xiao & Bowker, 2020). Thus, the role of biocrusts in affecting surface energy balance cannot be neglected. It is forecasted that in the next decades, dryland might suffer more severe droughts with less precipitation but higher temperature, and such climate change will certainly affect a range of ecosystem processes. Even small changes in temperature and moisture will influence thermal and moisture concentration gradients, which further drive large changes in soil vapor transport and alter the soil water regimes (Jabro, 2009; Guan et al., 2023). In our study, temperature was the main atmospheric driving factor of vapor diffusivity (Table 1). Accordingly, biocrusts induce more rapid movement of inward and outward vapor under warmer temperature in comparison with bare soil, thus increasing soil evaporation and condensation. This may be the case following temperature-induced vapor transport which may result in condensation following distillation (Kidron, Kronenfeld, et al., 2022), and as discussed earlier, this may also result in some atmospheric water interception by mosses (Kidron et al., 2002; S. L. Li, Xiao, et al., 2021). These processes may affect microorganism activation and biomineralization, such as of $CaCO_3$ (Lopez-Canfin et al., 2022), but, further studies are still needed in order to substantiate biocrusts' role in these processes.

In addition, this study evaluated the performance of biocrusts on vapor diffusion, evaporation, and adsorption at the plot scale of the Chinese Loess Plateau. We must acknowledge that it is difficult to quantitatively evaluate the contribution of biological components to the vapor transport separately from other mechanisms. Moreover, caution should be taken when applying our results to larger spatial scales (e.g., regional and even global scales) or for other drylands with arid climates. The soil type and texture could also influence vapor transport, which suggests that different results may be obtained for the colonization of biocrusts on more fine-grained soils. Therefore, further studies are still necessary to explore the biocrusts' role in vapor transport at larger spatiotemporal scales for a more comprehensive understanding of the way in which biocrusts modulate hydrological processes and thereby change water balance in global drylands.

5. Conclusions

In this study, we analyzed the differences in soil vapor diffusion properties, vapor adsorption capacity, and water evaporation of three types of biocrusts (cyano crusts, mixed crusts, and moss crusts) in comparison to bare soil under different atmospheric conditions. Our results showed that biocrusts significantly increased vapor diffusivity due to their higher porosity and lower bulk density. The results of vapor adsorption measurements illustrated that all types of biocrusts highly increased vapor adsorption amounts by >30%, and these increasing effects were pronouncedly obvious in moss crusts under high RH condition. The structural equation model showed that the driving factor of soil vapor adsorption was the clay content and specific surface area. Besides, the average evaporation rate and cumulative evaporation amount of biocrusts were 3%–46% and 10%–63% higher than for the bare soil, which is attributable to biocrust-induced effects on water holding capacity. The increased vapor diffusivity is mainly attributed to the modification of water molecules kinetic energy, vapor diffusion pathway, wind speed, and turbulent pumping. Consequently, biocrusts would accelerate the vapor diffusion, adsorption, and evaporation, as a consequence impact surface energy and water balance, which are vital in various soil ecohydrological and biochemical processes. Improved knowledge about the effects of biocrusts on soil water movement in dryland ecosystem can be useful to understand how these ecological systems may offset the negative impacts of land degradation and desertification.

Data Availability Statement

The data that support the findings of this study can be downloaded through the following URL: https://figshare.com/articles/dataset/Data_for_Soil_Water_Vapor_Transport_Based_on_Experiment/24441784 (https://doi.org/10.6084/m9.figshare.24441784).

Acknowledgments
This study was funded by the National Natural Science Foundation of China (Grant 42077010), the "Light of West China" Program of the Chinese Academy of Sciences (Grant 2019), and the Open Fund for Key Laboratory of Land Degradation and Ecological Restoration in Northwestern China of Ningxia University (Grant LDER2022Z02). The authors are grateful to the Shenmu Experimental Station of Soil Erosion and Environment, CAS & MOE for logistical support. Furthermore, the authors express their gratitude to Yanjia Zheng for assistance with data collection.

References

Akin, I. D., & Likos, W. J. (2017). Evaluation of isotherm models for water vapor sorption behavior of expansive clays. *Journal of Performance of Constructed Facilities*, *31*(1), D4016001. https://doi.org/10.1061/(ASCE)CF.1943-5509.0000899

Arthur, E. (2017). Rapid estimation of cation exchange capacity from soil water content. *European Journal of Soil Science*, *68*(3), 365–373. https://doi.org/10.1111/ejss.12418

Arthur, E., Tuller, M., Moldrup, P., & de Jonge, L. W. (2016). Evaluation of theoretical and empirical water vapor sorption isotherm models for soils. *Water Resources Research*, *52*(1), 190–205. https://doi.org/10.1002/2015WR017681

Arthur, E., Tuller, M., Moldrup, P., & de Jonge, L. W. (2020). Clay content and mineralogy, organic carbon and cation exchange capacity affect water vapour sorption hysteresis of soil. *European Journal of Soil Science*, *71*(2), 204–214. https://doi.org/10.1111/ejss.12853

Arthur, E., Tuller, M., Moldrup, P., Greve, M. H., Knadel, M., & de Jonge, L. W. (2018). Applicability of the Guggenheim-Anderson-Boer water vapour sorption model for estimation of soil specific surface area. *European Journal of Soil Science*, *69*(2), 245–255. https://doi.org/10.1111/ejss.12524

Arthur, E., Tuller, M., Moldrup, P., Jensen, D. K., & de Jonge, L. W. (2015). Prediction of clay content from water vapour sorption isotherms considering hysteresis and soil organic matter content. *European Journal of Soil Science*, *66*(1), 206–217. https://doi.org/10.1111/ejss.12191

Berdugo, M., Delgado-Baquerizo, M., Soliveres, S., Hernández-Clemente, R., Zhao, Y. C., Gaitán, J. J., et al. (2020). Global ecosystem thresholds driven by aridity. *Science*, *367*(6479), 787–790. https://doi.org/10.1126/science.aay5958

Beymer, R. J., & Klopatek, J. M. (1991). Potential contribution of carbon by microphytic crusts in pinyon-juniper woodlands. *Arid Soil Research and Rehabilitation*, *5*(3), 187–198. https://doi.org/10.1080/15324989109381279

Bisdom, E. B. A., Dekker, L. W., & Schoute, J. F. T. (1993). Water repellency of sieve fractions from sandy soils and relationships with organic material and soil structure. *Geoderma*, *56*(1–4), 105–118. https://doi.org/10.1016/0016-7061(93)90103-R

Bowker, M. A., Reed, S. C., Maestre, F. T., & Eldridge, D. J. (2018). Biocrusts: The living skin of the earth. *Plant and Soil*, *429*(1–2), 1–7. https://doi.org/10.1007/s11104-018-3735-1

Bu, C. F., Zhao, Y., Hill, R. L., Zhao, C. L., Yang, Y. S., Zhang, P., & Wu, S. F. (2015). Wind erosion prevention characteristics and key influencing factors of bryophytic soil crusts. *Plant and Soil*, *397*(1–2), 163–174. https://doi.org/10.1007/s11104-015-2609-z

Cahill, A. T., & Parlange, M. B. (1998). On water vapor transport in field soils. *Water Resources Research*, *34*(4), 731–739. https://doi.org/10.1029/97WR03756

Cass, A., Campbell, G. S., & Jones, T. L. (1984). Enhancement of thermal water vapor diffusion in soil. *Soil Science Society of America Journal*, *48*(1), 25–32. https://doi.org/10.2136/sssaj1984.03615995004800010005x

Chamizo, S., Cantón, Y., Rodríguez-Caballero, E., & Domingo, F. (2016). Biocrusts positively affect the soil water balance in semiarid ecosystems. *Ecohydrology*, *9*(7), 1208–1221. https://doi.org/10.1002/eco.1719

Chen, C., Arthur, E., Zhou, H., Wang, X., Shang, J. Y., Hu, K. L., & Ren, T. S. (2021). A new model for soil water vapor sorption isotherms considering adsorption and condensation. *Soil Science Society of America Journal*, *85*(2), 195–206. https://doi.org/10.1002/saj2.20181

Chen, C., Jiang, Y. J., Sun, B., Zhou, H., & Hallett, P. D. (2022). Organic manure and lime change water vapour sorption of a red soil by altering water repellency and specific surface area. *European Journal of Soil Science*, *73*(2), e13223. https://doi.org/10.1111/ejss.13223

Chen, N., Wang, X. P., Zhang, Y. F., Yu, K. L., & Zhao, C. M. (2018). Ecohydrological effects of biological soil crust on the vegetation dynamics of restoration in a dryland ecosystem. *Journal of Hydrology*, *563*, 1068–1077. https://doi.org/10.1016/j.jhydrol.2018.06.076

Chen, R. Y., Zhang, Y. M., Li, Y., Wei, W. S., Zhang, J., & Wu, N. (2009). The variation of morphological features and mineralogical components of biological soil crusts in the Gurbantunggut Desert of Northwestern China. *Environmental Geology*, *57*(5), 1135–1143. https://doi.org/10.1007/s00254-008-1410-1

Cheng, W., Hanna, K., & Boily, J. F. (2019). Water vapor binding on organic matter-coated minerals. *Environmental Science and Technology*, *53*(3), 1252–1257. https://doi.org/10.1021/acs.est.8b05134

Chenu, C. (1993). Clay-or sand-polysaccharide associations as models for the interface between micro-organisms and soil: Water related properties and microstructure. *Geoderma*, *56*, 143–156. https://doi.org/10.1016/B978-0-444-81490-6.50016-9

Chock, T., Antoninka, A. J., Faist, A. M., Bowker, M. A., Belnap, J., & Barger, N. N. (2019). Responses of biological soil crusts to rehabilitation strategies. *Journal of Arid Environments*, *163*, 77–85. https://doi.org/10.1016/j.jaridenv.2018.10.007

Danin, A., & Ganor, E. (1991). Trapping of airborne dust by mosses in the Negev Desert, Israel. *Earth Surface Processes and Landforms*, *16*(2), 153–162. https://doi.org/10.1002/esp.3290160206

de Amesti, P., de la Fuente, A., & Suarez, F. (2020). Evaporation from unsaturated soils as a function of the air and soil sides of the land surface. *Water Resources Research*, *56*(12), e2020WR028643. https://doi.org/10.1029/2020WR028643

Deb, S. K., Shukla, M. K., Sharma, P., & Mexal, J. G. (2011). Coupled liquid water, water vapor, and heat transport simulations in an unsaturated zone of a sandy loam field. *Soil Science*, *176*(8), 387–398. https://doi.org/10.1097/SS.0b013e318221f132

Deol, P., Heitman, J. L., Amoozegar, A., & Horton, R. (2012). Quantifying nonisothermal subsurface soil water evaporation. *Water Resources Research*, *48*(11), W11503. https://doi.org/10.1029/2012WR012516

Faist, A. M., Herrick, J. E., Belnap, J., van Zee, J. W., & Barger, N. N. (2017). Biological soil crust and disturbance controls on surface hydrology in a semi-arid ecosystem. *Ecosphere*, *8*(3), e01691. https://doi.org/10.1002/ecs2.1691

Felde, V. J. M. N. L., Drahorad, S. L., Felix-Henningsen, P., & Hoon, S. R. (2018). Ongoing oversanding induces biological soil crust layering – A new approach for biological soil crust structure elucidation determined from high resolution penetration resistance data. *Geoderma*, *313*, 150–264. https://doi.org/10.1016/j.geoderma.2017.11.022

Fick, A. (1855). Ueber diffusion. *Annalen der Physik*, *170*(1), 59–86. https://doi.org/10.1002/andp.18551700105

Fischer, T., Veste, M., Wiehe, W., & Lange, P. (2010). Water repellency and pore clogging at early successional stages of microbiotic crusts on inland dunes, Brandenburg, NE Germany. *Catena*, *80*(1), 47–52. https://doi.org/10.1016/j.catena.2009.08.009

Flemming, H., & Wingender, J. (2010). The biofilm matrix. *Nature Reviews Microbiology*, *8*(9), 623–633. https://doi.org/10.1038/nrmicro2415

Godinho, A. L., & Bhosle, S. (2009). Sand aggregation by exopolysaccharide-producing microbacterium arborescens–AGSB. *Current Microbiology*, *58*(6), 616–621. https://doi.org/10.1007/s00284-009-9400-4

Guan, C., Chen, N., Qiao, L. J., Ma, X. J., & Zhao, C. M. (2023). Biocrusts regulate the effect of rainfall pulses on soil respiration at different temporal scales on the Loess Plateau. *Soil Biology and Biochemistry*, *180*, 109018. https://doi.org/10.1016/j.soilbio.2023.109018

Guo, Q., Wang, Z. L., & Shen, N. (2023). Plot-based study to evaluate raindrop detachment capacity on moss-dominated biocrusted slope under simulated rainfall with different intensities. *Catena*, *226*, 107084. https://doi.org/10.1016/j.catena.2023.107084

Guo, Y. S., Furrer, J. M., Kadilak, A. L., Hinestroza, H. F., Gage, D. J., Cho, Y. K., & Shor, L. M. (2018). Bacterial extracellular polymeric substances amplify water content variability at the pore scale. *Frontiers in Environmental Science*, *6*, 93. https://doi.org/10.3389/fenvs.2018.00093

Heitman, J. L., Horton, R., Ren, T., Nassar, I. N., & Davis, D. D. (2008). A test of coupled soil heat and water transfer prediction under transient boundary temperatures. *Soil Science Society of America Journal*, *72*(5), 1197–1207. https://doi.org/10.2136/sssaj2007.0234

Heitman, J. L., Xiao, X., Horton, R., & Sauer, T. J. (2008). Sensible heat measurements indicating depth and magnitude of subsurface soil water evaporation. *Water Resources Research*, *44*(4), W00D05. https://doi.org/10.1029/2008WR006961

Heredia-Velásquez, A. M., Giraldo-Silva, A., Nelson, C., Bethany, J., Kut, P., González-de-Salceda, L., & Garcia-Pichel, F. (2023). Dual use of solar power plants as biocrust nurseries for large-scale arid soil restoration. *Nature Sustainability*, *6*(8), 955–964. https://doi.org/10.1038/s41893-023-01106-8

Huang, J. P., Yu, H. P., Guan, X. D., Wang, G. Y., & Guo, R. (2016). Accelerated dryland expansion under climate change. *Nature Climate Change*, *6*(2), 166–171. https://doi.org/10.1038/nclimate2837

IPCC. (2021). *Climate Change 2021: the Physical Science Basis. Contribution of Working Group I to the Sixth Assessment Report of the Intergovernmental Panel on Climate Change*. Cambridge University Press.

Jabro, J. D. (2009). Water vapor diffusion through soil as affected by temperature and aggregate size. *Transport in Porous Media*, *77*(3), 417–428. https://doi.org/10.1007/s11242-008-9267-z

Jester, W., & Klik, A. (2005). Soil surface roughness measurement-methods, applicability, and surface representation. *Catena*, *64*(2–3), 174–192. https://doi.org/10.1016/j.catena.2005.08.005

Jiang, Z. Y., Li, X. Y., Wei, J. Q., Chen, H. Y., Li, Z. C., Liu, L., & Hu, X. (2018). Contrasting surface soil hydrology regulated by biological and physical soil crusts for patchy grass in the high-altitude alpine steppe ecosystem. *Geoderma*, *326*, 201–209. https://doi.org/10.1016/j.geoderma.2018.04.009

Kakeh, J., Gorji, M., Mohammadi, M. H., Asadi, H., Khormali, F., & Sohrabi, M. (2021). Effect of biocrusts on profile distribution of soil water content and salinity at different stages of evaporation. *Journal of Arid Environments*, *191*, 104514. https://doi.org/10.1016/j.jaridenv.2021.104514

Karnieli, A., Kidron, G. J., Glaesser, C., & Ben Dor, E. (1999). Spectral characteristics of cyanobacteria soil crust in semiarid environments. *Remote Sensing of Environment*, *69*(1), 67–75. https://doi.org/10.1016/S0034-4257(98)00110-2

Kheirfam, H., & Roohi, M. (2020). Accelerating the formation of biological soil crusts in the newly dried-up lakebeds using the inoculation-based technique. *Science of the Total Environment*, *706*, 136036. https://doi.org/10.1016/j.scitotenv.2019.136036

Khorshidi, M., & Lu, N. (2017). Intrinsic relation between soil water retention and cation exchange capacity. *Journal of Geotechnical and Geoenvironmental Engineering*, *143*(4), 4016119. https://doi.org/10.1061/(ASCE)GT.1943-5606.0001633

Kidron, G. J. (2019). Biocrust research: A critical view on eight common hydrological-related paradigms and dubious theses. *Ecohydrology*, *12*(2), e2061. https://doi.org/10.1002/eco.2061

Kidron, G. J., Fischer, T., & Xiao, B. (2022). The ambivalent effect of biocrusts on evaporation: Can the contradictory conclusions be explained? A review. *Geoderma*, *416*, 115805. https://doi.org/10.1016/j.geoderma.2022.115805

Kidron, G. J., Herrnstadt, I., & Barzilay, E. (2002). The role of dew as a moisture source for sand microbiotic crusts in the Negev Desert, Israel. *Journal of Arid Environments*, *52*(4), 517–533. https://doi.org/10.1016/jare.2002.1014

Kidron, G. J., & Kronenfeld, R. (2023). One year-long evaluation of non-rainfall water available to soil biocrusts in the Negev Highlands. *Ecohydrology*, *16*(4), e2529. https://doi.org/10.1002/eco.2529

Kidron, G. J., Kronenfeld, R., Xiao, B., & Starinsky, A. (2022). Wet-dry cycles on sandy and loessial Negev soils: Implications for biocrust establishment and growth? *Ecohydrology*, *15*(2), e2379. https://doi.org/10.1002/eco.2379

Kidron, G. J., & Tal, S. Y. (2012). The effect of biocrusts on evaporation from sand dunes in the Negev Desert. *Geoderma*, *179–180*, 104–112. https://doi.org/10.1016/j.geoderma.2012.02.021

Kidron, G. J., Wang, Y., & Herzberg, M. (2020). Exoplosaccharides may increase biocrust rigidity and induce runoff generation. *Journal of Hydrology*, *588*, 125081. https://doi.org/10.1016/j.jhydrol.2020.125081

Kirschbaum, M. U., Giltrap, D. L., McNally, S. R., Liáng, L. L., Hedley, C. B., Moinet, G. Y., et al. (2020). Estimating the mineral surface area of soils by measured water adsorption. Adjusting for the confounding effect of water adsorption by soil organic carbon. *European Journal of Soil Science*, *71*(3), 382–391. https://doi.org/10.1111/ejss.12892

Lal, R., & Shukla, M. K. (2004). *Principles of soil physics*. CRC Press.

Lan, S. B., Wu, L., Zhang, D. L., & Hu, C. X. (2012). Successional stages of biological soil crusts and their microstructure variability in Shapotou region (China). *Environmental Earth Sciences*, *65*(1), 77–88. https://doi.org/10.1007/s12665-011-1066-0

Lange, O. L., Kidron, G. J., Büdel, B., Meyer, A., Killian, E., & Abeliovich, A. (1992). Taxonomic composition and photosynthetic characteristics of the "biological soil crusts" covering sand dunes in the Western Negev Desert. *Functional Ecology*, *6*(5), 519–527. https://doi.org/10.2307/2390048

Lehmann, A., Zheng, W., & Rillig, M. C. (2017). Soil biota contributions to soil aggregation. *Nature Ecology & Evolution*, *1*(12), 1828–1835. https://doi.org/10.1038/s41559-017-0344-y

Li, S. L., Bowker, M. A., & Xiao, B. (2021). Biocrusts enhance non-rainfall water deposition and alter its distribution in dryland soils. *Journal of Hydrology*, *595*, 126050. https://doi.org/10.1016/j.jhydrol.2021.12605

Li, S. L., Bowker, M. A., & Xiao, B. (2022a). Biocrust impacts on dryland soil water balance: A path toward the whole picture. *Global Change Biology*, *28*(21), 6462–6481. https://doi.org/10.1111/gcb.16416

Li, S. L., Bowker, M. A., & Xiao, B. (2022b). Impacts of moss-dominated biocrusts on rainwater infiltration, vertical water flow, and surface soil evaporation in drylands. *Journal of Hydrology*, *612*, 128176. https://doi.org/10.1016/j.jhydrol.2022.128176

Li, S. L., & Xiao, B. (2022). Cyanobacteria and moss biocrusts increase evaporation by regulating surface soil moisture and temperature on the northern Loess Plateau, China. *Catena*, *212*, 106068. https://doi.org/10.1016/j.catena.2022.106068

Li, S. L., Xiao, B., Sun, F. H., & Kidron, G. J. (2021). Moss-dominated biocrusts enhance water vapor sorption capacity of surface soil and increase non-rainfall water deposition in drylands. *Geoderma*, *388*, 114930. https://doi.org/10.1016/j.geoderma.2021.114930

Li, X. R., Hui, R., Tan, H. J., Zhao, Y., Liu, R. T., & Song, N. P. (2021). Biocrust research in China: Recent progress and application in land degradation control. *Frontiers in Plant Science*, *12*, 751521. https://doi.org/10.3389/fpls.2021.751521

Li, X. R., Jia, R. L., Zhang, Z. S., Zhang, P., & Hui, R. (2018). Hydrological response of biological soil crusts to global warming: A ten-year simulative study. *Global Change Biology*, *24*(10), 4960–4971. https://doi.org/10.1111/gcb.14378

Lichner, L., Holko, L., Zhukova, N., Shacht, K., Rajkai, K., Fodor, N., & Sándor, R. (2012). Plants and biological soil crust influence the hydrophysical parameters and water flow in an aeolian sandy soil. *Journal of Hydrology and Hyromechanics*, *60*(4), 309–318. https://doi.org/10.2478/v10098-012-0027-y

Liu, D. D., & She, D. L. (2020). Combined effects of moss crusts and pine needles on evaporation of carbonate-derived laterite from karst mountainous lands. *Journal of Hydrology*, *586*, 124859. https://doi.org/10.1016/j.jhydrol.2020.124859

Liu, L. C., Liu, Y. B., Hui, R., & Xie, M. (2017). Recovery of microbial community structure of biological soil crusts in successional stages of Shapotou desert revegetation, northwest China. *Soil Biology and Biochemistry*, *107*, 125–128. https://doi.org/10.1016/j.soilbio.2016.12.030

Lopez-Canfin, C., Lázaro, R., & Sánchez-Cañete, E. P. (2022). Water vapor adsorption by dry soils: A potential link between the water and carbon cycles. *Science of the Total Environment*, *824*, 153746. https://doi.org/10.1016/j.scitotenv.2022.153746

Lu, N., & Khorshidi, M. (2015). Mechanisms for soil–water retention and hysteresis at high suction range. *Journal of Geotechnical and Geoenvironmental Engineering*, *141*(8), 04015032. https://doi.org/10.1061/(ASCE)GT.1943-5606.0001325

Luo, R., Liu, Z. Y., Huang, T. T., & Tu, C. Z. (2018). Water vapor passing through asphalt mixtures under different relative humidity differentials. *Construction and Building Materials*, *165*, 920–930. https://doi.org/10.1016/j.conbuildmat.2018.01.047

Luo, R., & Tu, C. Z. (2019). Actual diffusivities and diffusion paths of water vapor in asphalt mixtures. *Construction and Building Materials*, *207*, 145–157. https://doi.org/10.1016/j.conbuildmat.2019.02.091

Mager, D. M., & Thomas, A. D. (2011). Extracellular polysaccharides from cyanobacterial soil crusts: A review of their role in dryland soil processes. *Journal of Arid Environments*, *75*(2), 91–97. https://doi.org/10.1016/j.jaridenv.2010.10.001

Maier, S., Tamm, A., Wu, D., Caesar, J., Grube, M., & Weber, B. (2018). Photoautotrophic organisms control microbial abundance, diversity, and physiology in different types of biological soil crusts. *ISME Journal*, *12*(4), 1032–1046. https://doi.org/10.1038/s41396-018-0062-8

Mao, D. H., Wang, Z. M., Wu, B. F., Zeng, Y., Luo, L., & Zhang, B. (2018). Land degradation and restoration in the arid and semiarid zones of China: Quantified evidence and implications from satellites. *Land Degradation and Development*, *29*(11), 3841–3851. https://doi.org/10.1002/ldr.3135

Menon, M., Yuan, Q., Jia, X., Dougill, A. J., Hoon, S. R., Thomas, A. D., & Williams, R. A. (2011). Assessment of physical and hydrological properties of biological soil crusts using X-ray microtomography and modeling. *Journal of Hydrology*, *397*(1–2), 47–54. https://doi.org/10.1016/j.jhydrol.2010.11.021

Merced, A., & Renzaglia, K. S. (2017). Structure, function and evolution of stomata from a bryological perspective. *Bryophyte Diversity and Evolution*, *39*(1), 7–20. https://doi.org/10.11646/bde.39.1.4

Mücher, H. J., Chartres, C. J., Tongway, D. J., & Greene, R. S. B. (1988). Micromorphology and significance of the surface crusts of soils in rangelands near Cobar, Australia. *Geoderma*, *42*(3–4), 227–244. https://doi.org/10.1016/0016-7061(88)90003-1

Nejidat, A., Potrafka, R. M., & Zaady, E. (2016). Successional biocrust stages on dead shrub soil mounds after severe drought: Effect of micro-geomorphology on microbial community structure and ecosystem recovery. *Soil Biology and Biochemistry*, *103*, 213–220. https://doi.org/10.1016/j.soilbio.2016.08.028

Newman, A. (1983). The specific surface of soils determined by water sorption. *Journal of Soil Science*, *34*(1), 23–32. https://doi.org/10.1111/j.1365-2389.1983.tb00809.x

Parlange, M. B., Cahill, A. T., Nielsen, D. R., Hopmans, J. W., & Wendroth, O. (1998). Review of heat and water movement in field soils. *Soil and Tillage Research*, *47*(1–2), 5–10. https://doi.org/10.1016/S0167-1987(98)00066-X

Peng, J., Wu, X. L., Ni, S. M., Wang, J. G., Song, Y. T., & Cai, C. F. (2022). Investigating intra-aggregate microstructure characteristics and influencing factors of six soil types along a climatic gradient. *Catena*, *210*, 105867. https://doi.org/10.1016/j.catena.2021.105867

Penman, H. L. (1940). Gas and vapor movements in soil: I. The diffusion of vapors through porous solids. *Journal of Agricultural Science*, *30*(3), 437–462. https://doi.org/10.1017/S0021859600048164

Qiu, D. X., Bowker, M. A., Xiao, B., Zhao, Y. G., Zhou, X. B., & Li, X. R. (2023). Mapping biocrust distribution in China's drylands under changing climate. *Science of the Total Environment*, *905*, 167211. https://doi.org/10.1016/j.scitotenv.2023.167211

Quirk, J., & Murray, R. (1999). Appraisal of the ethylene glycol monoethyl ether method for measuring hydratable surface area of clays and soils. *Soil Science Society of America Journal*, *63*(4), 839–849. https://doi.org/10.2136/sssaj1999.634839x

Reynolds, J. F., Smith, D. M. S., Lambin, E. F., Turner II, B. L., Mortimore, M., Batterbury, S. P. J., et al. (2007). Global desertification: Building a science for dryland development. *Science*, *316*(5826), 847–851. https://doi.org/10.1126/science.1131634

Reynolds, R., Belnap, J., Reheis, M., Lamothe, P., & Luiszer, F. (2001). Aeolian dust in Colorado Plateau soils: Nutrient inputs and recent change in source. *Proceedings of the National Academy of Sciences*, *98*(13), 7123–7127. https://doi.org/10.1073/pnas.121094298

Rodríguez-Caballero, E., Aguilar, M. A., Cantón, Y., Chamizo, S., & Aguilar, F. J. (2015). Swelling of biocrusts upon wetting induces changes in surface micro-topography. *Soil Biology and Biochemistry*, *82*, 1–5. https://doi.org/10.1016/j.soilbio.2014.12.010

Rodríguez-Caballero, E., Belnap, J., Büdel, B., Crutzen, P. J., Andreae, M. O., Pöschl, U., & Weber, B. (2018). Dryland photoautotrophic soil surface communities endangered by global change. *Nature Geoscience*, *11*(3), 185–189. https://doi.org/10.1038/s41561-018-0072-1

Rossi, F., Mugnai, G., & De Philippis, R. (2018). Complex role of the polymeric matrix in biological soil crusts. *Plant and Soil*, *429*(1–2), 19–34. https://doi.org/10.1007/s11104-017-3441-4

Rossi, F., Potrafka, R. M., Garcia Pichel, F., & De Philippis, R. (2012). The role of the exopolysaccharides in enhancing hydraulic conductivity of biological soil crusts. *Soil Biology and Biochemistry*, *46*, 33–40. https://doi.org/10.1016/j.soilbio.2011.10.016

Rutherford, W. A., Painter, T. H., Ferrenberg, S., Belnap, J., Okin, G. S., Flagg, C., & Reed, S. C. (2017). Albedo feedbacks to future climate via climate change impacts on dryland biocrusts. *Scientific Reports*, *7*(1), 44188. https://doi.org/10.1038/srep44188

Schneider, M., & Goss, K. U. (2012). Prediction of the water sorption isotherm in air dry soils. *Geoderma*, *170*, 64–69. https://doi.org/10.1016/j.geoderma.2011.10.008

Smits, K. M., Ngo, V. V., Cihan, A., Sakaki, T., & Illangasekare, T. H. (2012). An evaluation of models of bare soil evaporation formulated with different land surface boundary conditions and assumptions. *Water Resources Research*, *48*(12), W12526. https://doi.org/10.1029/2012WR012113

Song, X., Chen, C., Arthur, E., Tuller, M., Zhou, H., Shang, J. Y., & Ren, T. S. (2022). Cation exchange capacity and soil pore system play key roles in water vapour sorption. *Geoderma*, *424*, 116017. https://doi.org/10.1016/j.geoderma.2022.116017

Souza-Egipsy, V., Wierzchos, J., Sancho, C., Belmonte, A., & Ascaso, C. (2004). Role of biological soil crust cover in bioweathering and protection of sandstones in a semiarid landscape (Torrollones de Gabarda, Huesca, Spain). *Earth Surface Processes and Landforms*, *29*(13), 1651–1661. https://doi.org/10.1002/esp.1118

Sun, F. H., Xiao, B., & Kidron, G. J. (2022). Towards the influences of three types of biocrusts on soil water in drylands: Insights from horizontal infiltration and soil water retention. *Geoderma*, *428*, 116136. https://doi.org/10.1016/j.geoderma.2022.116136

Sun, F. H., Xiao, B., Kidron, G. J., & Heitman, J. L. (2022). Insights about biocrust effects on soil gas transport and aeration in drylands: Permeability, diffusivity, and their connection to hydraulic conductivity. *Geoderma*, *427*, 116137. https://doi.org/10.1016/j.geoderma.2022.116137

Sun, F. H., Xiao, B., Kidron, G. J., & Markus, T. (2023). Towards the effects of moss-dominated biocrusts on surface soil aeration in drylands: Air permeability analysis and modeling. *Catena*, *223*, 106942. https://doi.org/10.1016/j.catena.2023.106942

Sun, F. H., Xiao, B., Li, S. L., & Kidron, G. J. (2021). Towards moss biocrust effects on surface soil water holding capacity: Soil water retention curve analysis and modeling. *Geoderma*, *399*, 115120. https://doi.org/10.1016/j.geoderma.2021.115120

Sun, F. H., Xiao, B., Li, S. L., Yu, X. X., Kidron, G. J., & Heitman, J. (2023). Direct evidence and mechanism for biocrusts-induced improvements in pore structure of dryland soil and the hydrological implications. *Journal of Hydrology*, *623*, 129846. https://doi.org/10.1016/j.jhydrol.2023.129846

Thomas, A. D., & Dougill, A. J. (2007). Spatial and temporal distribution of cyanobacterial soil crusts in the Kalahari: Implications for soil surface properties. *Geomorphology*, *85*(1–2), 17–29. https://doi.org/10.1016/j.geomorph.2006.03.029

Tuller, M., Or, D., & Dudley, L. M. (1999). Adsorption and capillary condensation in porous media: Liquid retention and interfacial configurations in angular pores. *Water Resources Research*, *35*(7), 1949–1964. https://doi.org/10.1029/1999WR900098

Verrecchia, E., Yair, A., Kidron, G. J., & Verrecchia, K. (1995). Physical properties of the psammophile cryptogamic crust and their consequences to the water regime of sandy soils, North-western Negev Desert, Israel. *Journal of Arid Environments*, *29*(4), 427–437. https://doi.org/10.1016/S0140-1963(95)80015-8

Wang, L. L., Wang, L. F., Ren, X. M., Ye, X. D., Li, W. W., Yuan, S. J., et al. (2012). pH dependence of structure and surface properties of microbial EPS. *Environmental Science & Technology*, *46*(2), 737–744. https://doi.org/10.1021/es203540w

Weber, B., Belnap, J., Büdel, B., Antoninka, A., Barger, N., Chaudhary, V., et al. (2022). What is a biocrust? A refined, contemporary definition for a broadening research community. *Biological Reviews*, *97*(5), 1768–1785. https://doi.org/10.1111/brv.12862

Xiao, B., & Bowker, M. A. (2020). Moss-biocrusts strongly decrease soil surface albedo, altering land-surface energy balance in a dryland ecosystem. *Science of the Total Environment*, *741*, 140425. https://doi.org/10.1016/j.scitotenv.2020.140425

Xiao, B., Bowker, M., Zhao, Y. G., Chamizo, S., & Issa, O. M. (2022). Biocrusts: Engineers and architects of surface soil properties, functions, and processes in dryland ecosystems. *Geoderma*, *424*, 116015. https://doi.org/10.1016/j.geoderma.2022.116015

Xiao, B., Ma, S., & Hu, K. L. (2019). Moss biocrusts regulate surface soil thermal properties and generate buffering effects on soil temperature dynamics in dryland ecosystem. *Geoderma*, *351*, 9–24. https://doi.org/10.1016/j.geoderma.2019.05.017

Xiao, B., Sun, F. H., Hu, K. L., & Kidron, G. J. (2019). Biocrusts reduce surface soil infiltrability and impede soil water infiltration under tension and ponding conditions in dryland ecosystem. *Journal of Hydrology*, *568*, 792–802. https://doi.org/10.1016/j.jhydrol.2018.11.051

Xiao, B., Sun, F. H., Yao, X. M., Hu, K. L., & Kidron, G. J. (2019). Seasonal variations in infiltrability of moss-dominated biocrusts on aeolian sand and loess soil in the Chinese Loess Plateau. *Hydrological Processes*, *33*(18), 2449–2463. https://doi.org/10.1002/hyp.13484

Xiao, B., Zhao, Y., Wang, H., & Wu, J. (2014). Natural recovery of moss-dominated biological soil crusts after surface soil removal and their long-term effects on soil water conditions in a semi-arid environment. *Catena*, *120*, 1–11. https://doi.org/10.1016/j.catena.2014.03.018

Xiao, B., Zhao, Y. G., & Shao, M. A. (2010). Characteristics and numeric simulation of soil evaporation in biological soil crusts. *Journal of Arid Environments*, *74*(1), 121–130. https://doi.org/10.1016/j.jaridenv.2009.06.013

Yamanaka, T., Takeda, A., & Shimada, J. (1998). Evaporation beneath the soil surface: Some observational evidence and numerical experiments. *Hydrological Processes*, *12*(13–14), 2193–2203. https://doi.org/10.1002/(SICI)1099-1085(19981030)12:13/14<2193::AID-HYP729>3.0.CO;2-P

Zhai, X. F., & Horn, R. (2018). Effect of static and cyclic loading including spatial variation caused by vertical holes on changes in soil aeration. *Soil and Tillage Research*, *177*, 61–67. https://doi.org/10.1016/j.still.2017.11.008

Zhang, Y. M., Wang, H. L., Wang, X. Q., Yang, W. K., & Zhang, D. Y. (2006). The microstructure of microbiotic crust and its influence on wind erosion for a sandy soil surface in the Gurbantunggut Desert of Northwestern China. *Geoderma*, *132*(3–4), 441–449. https://doi.org/10.1016/j.geoderma.2005.06.008